*Russian Chemical Reviews* **73** (4) 351 – 370 (2004) © 2004 Russian Academy of Sciences and Turpion Ltd

DOI 10.1070/RC2004v073n04ABEH000768

# The theory of formation of surface complexes and its application to the description of multicomponent dynamic sorption systems

W H Höll, A I Kalinitchev

## Contents


| | | |
|---|---|---|
| I. | Introduction | 351 |
| II. | Uptake of ions due to protonation/dissociation reactions of surface groups | 352 |
| III. | Uptake of ions due to Lewis acid/Lewis base interactions | 355 |
| IV. | Evaluation of the SCT model parameters from experimental data | 356 |
| V. | Calculations of multicomponent equilibria using the SCT model | 360 |
| VI. | Application of the SCT model to nonlinear theory of multicomponent sorption dynamics and chromatography | 362 |
| VII. | Steady-state binary concentration distributions | 364 |
| VIII. | Computerised description of ion exchange dynamics in multicomponent systems using the SCT model | 364 |
| IX. | Modelling of the dynamics of ion exchange due to Lewis acid/Lewis base interactions, as applied to multicomponent systems | 365 |
| X. | Dynamics of ion exchange in multicomponent systems with allowance for ion complexation in the mobile liquid phase | 366 |
| XI. | Conclusion | 368 |


**Abstract. The fundamentals of the theory of formation of surface complexes (or the surface complexation theory, SCT), which is used in processing the results of studies on the equilibria in multicomponent ion exchange sorption systems, are outlined. The advantage of the theory is the use of the sorption characteristics of binary ion exchange systems for the description and calculation of multicomponent equilibria with allowance for the medium pH value. The solutions to some problems of nonlinear sorption dynamics theory obtained using the description of multicomponent equilibria in the framework of the SCT model are considered. Experimental data on the concentration distributions of components in frontal and displacement chromatograms are compared with the results of corresponding numerical calculations using various sets of parameters of the SCT model (including versions with allowance for the effect of complexation reactions in the mobile phase). The bibliography includes 88 references.**

## I. Introduction

The aim of this review is to highlight a recently developed model for the description of multicomponent ion exchange equilibria and its applications to nonlinear sorption dynamics theory. The model is called the theory of formation of surface complexes (or the surface complexation theory, SCT), because it assumes that near the surface of a sorbent (ion exchanger) each kind of counterion is located in the form of a surface complex within an individual Stern layer. Application of the SCT approach to nonlinear theory of multicomponent sorption dynamics and chromatography is a specific, complicated theoretical problem, which is solved by the authors of this review.

In the text below we will briefly outline a number of earlier models for the description of sorption phenomena (in some cases, with consideration of surface ion complexation).

Inorganic and organic ion exchange sorbents consist of either a crystalline or a polymeric matrix and various functional groups. Depending on the pH value of the solution contacting the ion exchanger, functional groups can be protonated or dissociated. Therefore, such sorbents can interact with ions in the liquid phase. As a result, sorption of ions at the surface of the ion exchanger becomes possible.[1] The surface charges produce an electric field directed normal to the surface. Consideration of the resulting electrostatic interactions led to development of various models for the description of sorption equilibria.[2–5]

Helmholtz postulated [1] that the surface charges are compensated by counterions which are located within an ordered (outer Helmholtz) layer some distance from the sorbent surface. The distribution of counterions is governed by the degree of hydration of the solute molecules. Gouy and Chapman [3,4] treated counterions as mass points randomly distributed over a diffusion layer. In this model, the corresponding electrostatic potential and charge density are described by the Poisson equation.

Later, Stern [5] used a combination of the two approaches mentioned above. He assumed that a fraction of counterions is located within an ordered layer near the sorbent surface, while the rest of the counterions are distributed over the neighbouring diffusion layer. The Stern model included finite sizes and thermal motion of hydrated ions.

Modern models consider not only electrostatic interactions but also chemical interactions (solvation of metal ions,[6–8] protonation of ligands,[9] adsorption) and a specific interaction between protons and hydroxyl ions.[10]

Yet another theoretical approach treats the adsorption of counterions as a result of (mainly) chemical interactions between functional groups located on the sorbent surface and dissolved species. Sorption of protons (or other ions) is considered as a local equilibrium established as a result of corresponding reactions. Specific (in the case of protons and hydroxyl ions) and nonspecific (for other ions) interactions cause the formation of ion

**W H Höll** Institute for Technical Chemistry, Karlsruhe Research Centre, PO Box 3640, D-76021 Karlsruhe, Helmholtz-Platz, Germany.
Fax (49-724) 782 23 77. E-mail: wolfgang.hoell@itc.frk.de
**A I Kalinitchev** Institute of Physical Chemistry, Russian Academy of Sciences, Leninsky prosp. 31, 119991 Moscow, Russian Federation.
Fax (7-095) 952 53 08. Tel. (7-095) 955 44 05.
E-mail: kalina@phyche.ac.ru

Received 23 September 2002
*Uspekhi Khimii* **73** (4) 383 – 403 (2004); translated by A M Raevsky

pairs at the sorbent surface, which can be treated as various types [1,2] of surface complexes.[11]

In this case, to include the additional contribution of electrostatic interactions to the adsorption,[7,8,12–16] one should know the electric capacitance of the sorbent. This parameter is usually unknown; therefore, a constant ion exchanger capacity model [15,17,18] is employed. Detailed consideration of this model can be found in the literature.[12,19,20]

Spectroscopic studies of the surfaces of ion exchangers revealed [21] that correct description of the adsorption of counterions requires a sorption model with more than one near-surface ion layer to be used. This led to the development [12,22,23] of a triple-layer model with the sorbent surface, β-plane and the diffusion layer as the first, second and third layers, respectively. In the framework of this model counterions can be adsorbed on both the outer layer (β-plane) and the inner layer (sorbent surface).

The surface adsorption of counterions on ion exchange resins was studied [24] using the Gouy–Chapman model [3,4] taking a weakly functionalised Amberlite XAD-2 resin as an example. Applicability of the SCT approach to the description of individual properties of different types of sorption sites was first appreciated by Horst [25] who used the triple-layer model to describe the ion exchange equilibrium on commercially available weakly acid resins.

Initially, the SCT model was developed only for weakly acid polymeric ion exchangers.[25] Further stages of its development and application to the quantitative description of ion equilibria in various organic ion exchange materials have been well documented.[26–36] In this model individual sorption layers are credited to each kind of counterion. Then, the model was extended to other ion exchange systems and currently it permits the description of pure cation or anion exchange equilibria [26,29,36] on various resins [27,28,35] and activated alumina and carbons,[30–32,36] as well as of the adsorption of heavy metal salts.[33,34]

The basic SCT model assumptions and the results obtained by applying the model to the description of equilibria in various multicomponent ion exchange systems including different types of ion exchangers [25–36] are presented in Sections II–V.

The use of the SCT approach appeared to be rather fruitful for solving a number of problems of nonlinear dynamics of multicomponent ion exchange sorption.[37–53] Methods for solution of these theoretical problems with consideration of equilibria using the SCT model as well as the results obtained are described in Sections VI–X.

# II. Uptake of ions due to protonation/dissociation reactions of surface groups

## 1. Simplified description of reactions on charged surfaces of amphoteric ion exchange resins

In deriving mathematical relationships of the surface complexation theory we will consider an idealised planar sorbent surface containing OH groups as sorption sites. We also assume that the sorption sites are uniformly distributed over the sorbent surface.[26,27] In liquid-phase systems the surface OH groups can be protonated in two ways.

In acid media the sorbent surface ($S$) containing the OH functional groups can be protonated following the reaction

$$S-OH + H^+ \rightleftharpoons S-OH_2^+. \quad (1)$$

To meet the condition for electroneutrality, the positive charge of the surface must be balanced by the negative charge of an anion (*e.g.*, $Cl^-$ ion)

$$S-OH_2^+ + Cl^- \rightleftharpoons S-OH_2Cl. \quad (2)$$

From Eqns (1) and (2) it follows that sorption of acids can occur in sufficiently acid media similarly to the uptake of acids with weakly basic ion exchangers.

In alkaline solutions the surface hydroxy groups can dissociate and release protons to the liquid phase

$$S-OH \rightleftharpoons S-O^- + H^+. \quad (3)$$

The negative surface charges must be compensated by the positive charges of, *e.g.*, $Na^+$ cations

$$S-O^- + Na^+ \rightleftharpoons S-ONa. \quad (4)$$

Taken together, Eqns (3) and (4) describe a cation exchange on an arbitrary cation exchanger.[30,31,36]

Each protolysis model mentioned above holds for the description of the uptake of acids or the exchange of protons for other monovalent cations in arbitrary pure anion or cation exchange processes. If the equilibrium state is considered for amphoteric ion exchangers and a liquid phase containing various cations and anions, the uptake of anions will decrease with an increase in the pH value until sorption is completely suppressed. The exchange of protons for cations increases in the same way. The pH regions of almost exclusive sorption of cations (or anions) are separated by the region corresponding to the maximum possible concentration of neutral surface groups. In this transient region, sorption of both cations and anions occurs, resulting in coverage of the surface with equal amounts of chemical equivalents of positively and negatively charged counterions.[30,31,36]

## 2. Basic SCT model assumptions

During the protonation or dissociation of the surface OH groups either a positive or negative electrostatic potential is generated, which depends on the pH value and on the ionic strength of the liquid phase. Due to the sorption of counterions at functional groups this potential is decreased. The SCT model assumes that each kind of counterion ($i$) is located at a characteristic distance from the surface. Therefore, ordered electrical double layers of Stern layers (1, ..., $i$, ... , $N$) are formed near the surface. The layer sequence begins at the sorbent surface: $S|1|...|i|...|j|...|N|D$, where $D$ is the most distant diffusion layer. The excess surface charge is balanced by the charges of counterions in the diffusion layer, which also contains co-ions (Fig. 1 *a*).[26–36]

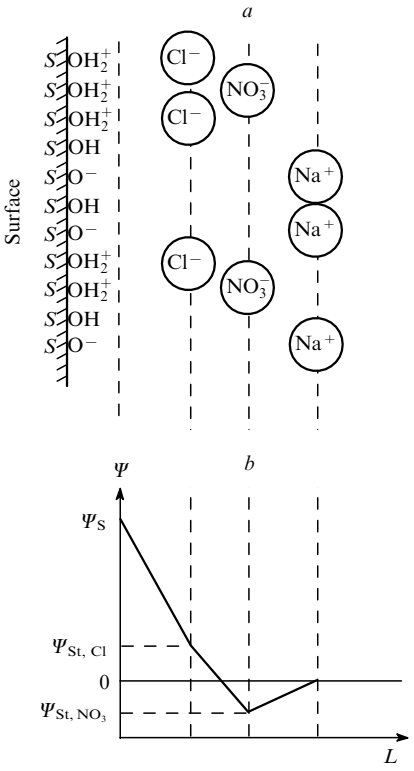



**Figure 1.** Stern layers (St) near an amphoteric surface (*a*) and the plot of electrostatic potential $\Psi$ *vs.* distance, $L$, from the surface of sorbent (*b*).[30]

As a consequence, the electrostatic potential $\Psi$ continuously decreases along the normal to the surface. The arrangement of counterions and the potential distribution within the Stern layers and within the diffusion layer for different types of ion exchangers have been well documented (see, *e.g.*, Refs 26–28, 30, 31, 34, 36). The arrangement of counterions and co-ions within the Stern layers is schematically depicted in Fig. 1 *a* and the corresponding electrostatic potential distribution for a solution containing $Cl^-$, $NO_3^-$ and $Na^+$ ions is shown in Fig. 1 *b*. The $\Psi(L)$ dependence between the layers $i|(i+1)$ is linear, because each electrical double layer is an electric capacitor of capacitance $C(i, i+1)$. The ions sorbed within the layers $1|...|j|...|N$ form a system of capacitors connected in series. The potential distribution in the diffusion layer $D$ (this layer is not shown in Fig. 1) is described by the Poisson – Boltzmann equation [26–31, 36] and the potential reaches a zero value in the liquid phase (see Fig. 1 *b*).

The equilibrium between the solid and liquid phases is mainly governed by protolytic reactions (1)–(4). Therefore, it is protons ($H^+$) sorbed at the surface that are responsible for the electrostatic potential. It is assumed that the anion rather than the cation layers are located closer to the surface (see Fig. 1 *a*).

## 3. Sorption equilibrium relationships in the SCT model

### a. General assumptions

The equilibrium relationships in the SCT model were derived assuming that

— functional groups are uniformly distributed across a planar surface;

— activity coefficients in the ion exchanger phase equal unity;

— any ion exchange is treated as replacement of a surface complex by a new one [as a consequence, the charge of the surface sorption sites ($z_R$) is defined as the least common multiple of the charges of the counterions involved in the exchange process].

### b. Surface reactions

Let us consider the derivation of the equilibrium relationships taking a simple system containing $Cl^-$ and $Na^+$ ions as an example (for the arrangement of the Stern sorption layers, see Fig. 1 *a* except for the $NO_3^-$ ions). The protolytic reactions (1) and (3) at the surface can be described using the mass action law (the corresponding expressions contain the local equilibrium constants). For instance, the protonation and dissociation/neutralisation reactions are characterised by the following constants:[30, 31, 36]

protonation [reaction (1)]

$$K_H^+ = \frac{c(S{-}OH_2^+)}{c(H^+)_{St}\, c(S{-}OH)}, \tag{5}$$

dissociation/neutralisation [reaction (3)]

$$K_H^- = \frac{c(S{-}OH)}{c(S{-}O^-)\, c(H^+)_{St}}. \tag{6}$$

The sorption of counterions ($Cl^-$ and $Na^+$) is considered in a similar way:[30, 31, 36]

sorption of anions [reaction (2)]

$$K_{Cl}^- = \frac{c(S{-}OH_2Cl)}{c(S{-}OH_2^+)\, c(Cl^-)_{St}}, \tag{7}$$

sorption of cations [reaction (4)]

$$K_{Na}^+ = \frac{c(S{-}ONa)}{c(S{-}O^-)\, c(Na^+)_{St}}. \tag{8}$$

The subscript St denotes the corresponding Stern sorption layer. The unknown concentrations, $c(i)_x$, of the component $i$ at a point $x$ of the electric field within the sorption layers are excluded from consideration. They are expressed *via* the experimentally determined liquid-phase concentrations [$c(i)$, mol litre$^{-1}$] using the Poisson – Boltzmann relationship [26–28, 30, 31, 36]

$$c(i)_x = c(i)\exp\left[-\frac{z(i)F}{RT}\Psi_x\right], \tag{9}$$

where F is the Faraday constant (in C kmol$^{-1}$) and $\Psi_x$ is the electrostatic potential at the distance $x$ from the sorbent surface (in volts).

The sorption of anions (in this case, chloride ions) includes the sorption of protons [see Eqn (1)] followed by the sorption of chloride ions [see Eqn (2)]. Since we have a sequence of reactions (1) and (2), the equilibrium constant for this process in the $S{-}OH_2^+$ portions (see Fig. 1 *a*) is given by [30, 31, 36]

$$K_{Cl}^H = K_H^+ K_{Cl}^-. \tag{10}$$

The uptake of cations (in this case, $Na^+$) develops as the competitive sorption of protons and sodium ions. As a consequence, the equilibrium constant for cation exchange equals the ratio of the corresponding individual equilibrium constants given by expressions (6) and (8) (see Refs 30, 31, 36)

$$K_{Na}^H = \frac{K_H^-}{K_{Na}^+}. \tag{11}$$

Using Eqns (5)–(11), we get [30, 31]

$$K_{Cl}^H = \frac{c(S{-}OH_2Cl)}{c(S{-}OH)c(Cl^-)c(H^+)}\exp\left[\frac{F}{RT}(\Psi_S - \Psi_{Cl})\right], \tag{12}$$

$$K_{Na}^H = \frac{c(S{-}OH)c(Na^+)}{c(S{-}ONa)c(H^+)}\exp\left[\frac{F}{RT}(\Psi_S - \Psi_{Na})\right], \tag{13}$$

where $\Psi_S$ is the electrostatic potential of the sorbent surface (in Volts).

It was shown [30, 31, 36] that the concentrations of the surface complexes, $c(S{-}Oi)$, are converted into solid-phase loadings $q(i)$ (in mg-equiv g$^{-1}$) of the sorbent, namely, $q$(OH), $q(Cl^-)$ and $q(Na^+)$ [$q$(OH) denotes the surface groups which remain undissociated and unprotonated].

Therefore, the pre-exponents in relationships (12) and (13) contain exclusively those quantities which can be determined experimentally. In the SCT model both expressions are called the generalised separation factors ($Q_j^i$) (see Refs 26–36). After introducing dimensionless sorbent loadings

$$y(i) = \frac{q(i)}{q_{max}}, \tag{14}$$

where $q_{max}$ is the maximum loading, the coefficients $Q_j^i$ are given by:[30, 31, 36]

$$Q_{Cl}^H = \frac{q(Cl^-)}{q(HO^-)c(H^+)c(Cl^-)} = \frac{y(Cl)}{y(HO^-)c(H^+)c(Cl^-)},$$
$$Q_{Na}^H = \frac{q(HO^-)c(Na^+)}{q(Na^+)c(H^+)} = \frac{y(HO^-)c(Na^+)}{y(Na^+)c(H^+)}. \tag{15}$$

Similar relationships can be derived for any monovalent counterions.

### c. Binary parameters

The electrostatic potential differences in Eqns (12) and (13) can be expressed *via* the surface charge densities in the series of electric capacitors formed by the Stern layers, *via* the charge densities in the diffusion layer [26–28] and *via* the loadings, $y(i)$, of the amphoteric sorbent surface with $Cl^-$ and $Na^+$ ions.[30, 31, 36] Mathematical treatment of the corresponding equations in the framework of

the SCT approach gives the following expressions for the generalised separation factors:[30,31,36]

$$\log Q^{H}_{Cl} = \log K^{H}_{Cl} + m(H,Cl)[-y(Cl) + y(Na)], \quad (16)$$

$$\log Q^{H}_{Na} = \log K^{H}_{Na} + m(H,Cl)y(Cl) + m(H,Na)y(Na). \quad (17)$$

The parameters $m(H,i)$ in Eqns (16) and (17) depend on the electric capacitance [$C(S,i)$, in F m$^{-2}$] of the capacitor formed by the sorbent surface and the corresponding Stern layer ($i$). They are defined as follows[26–31,36]

$$m(H,i) = \frac{1}{\ln 10}\frac{z_R q_{max} F^2}{A_0 C(S,i) RT}, \quad (18)$$

where $A_0$ (in m$^2$ g$^{-1}$) is the specific surface area of the sorbent, $z_R < 0$ for cation exchangers and $z_R > 0$ for anion exchangers. For binary exchange the numerical value of the parameter $z_R$ equals the least common multiple of the charges of two counterions.[30,31,36]

The general relationship of the SCT model for a system containing an arbitrary number of monovalent counterions can be deduced from similar considerations. For the component $i$ it has the form[30,31,36]

$$\log Q^{H}_{i} = \log K^{H}_{i} + \sum_{j=2}^{i-1}[m(H,j)V(j)y(j)] + m(H,i)\sum_{i}^{n} V(i)y(i). \quad (19)$$

Here $i$ and $j$ are the indices of counterions ($i = 2, 3, ..., n$; $j = 2, 3, ..., i-1$); $i = 1$ corresponds to hydrogen ions; and $V(j)$ and $V(i)$ are the signs of the charges of the counterions, namely, $V(i) = -1$ for anions and $V(j) = +1$ for cations.

For a given component $i$ the second term in expression (19) describes summation of the parameters for those counterions $j$, which in these Stern layers are located closer to the surface than the species $i$. The third term comprises the parameters for the counterions located at longer distances from the surface than the ions $i$. For an ion exchange system containing $n$ counterions there are $n-1$ equations of the type (19).

It is of great importance that all binary parameters of the SCT model $\{\log K^{H}_{i}; m(H,i)\}$ from $i = 2$ on can be successively evaluated from the experimental data for binary exchanges. Since in the framework of the SCT approach all equilibria are calculated using these pairs of binary parameters, the equilibrium constants for multicomponent ion exchange systems can be determined in a similar way. Some examples of calculations of multicomponent equilibria using the SCT model are given below.

### d. Extension to systems containing mixtures of monovalent and multivalent counterions

During the exchange of a divalent counterion for two monovalent counterions the divalent species replaces two adjacent ions at the surface. If the liquid phase contains one kind of divalent ions to be exchanged for the monovalent ions initially present in the sorbent, it is necessary that the sorbent have divalent sorption sites. They can be formed by two monovalent sites. As a consequence, two types of surface complexes, namely, two monovalent counterions (*e.g.*, $Cl^-$) — two monovalent sites (type $a$) and divalent counterion (*e.g.*, $SO_4^{2-}$) — two monovalent sites (type $b$) exist and exchange near the surface.

For a system containing $H^+$, $Na^+$, $Cl^-$ and $SO_4^{2-}$ counterions the generalised separation factors are given by the following expressions:[30,31,36]

for exchange of $SO_4^{2-}$ anions involving protonation [see Eqns (1) and (2)] and the formation of a complex of the type $b$

$$Q^{H}_{II\,SO_4} = \frac{c[(S{-}OH_2^+)_2{=}SO_4^{2-}]}{c(S{-}OH, S{-}OH)[c(H^+)]^2 c(SO_4^{2-})}; \quad (20)$$

for exchange of $Cl^-$ anions involving protonation [see Eqns (1) and (2)] and the formation of a complex of the type $a$

$$Q^{H}_{II\,Cl} = \frac{c(S{-}OH_2Cl, S{-}OH_2Cl)}{c(S{-}OH, S{-}OH)[c(H^+)]^2[c(Cl^-)]^2}; \quad (21)$$

for $Na^+/H^+$ exchange and the formation of a complex of the type $a$

$$Q^{H}_{II\,Na} = \frac{c(S{-}OH, S{-}OH)}{c(S{-}ONa, S{-}ONa)[c(H^+)]^2}. \quad (22)$$

The subscript 'II' means that expressions (20)–(22) were derived assuming the presence of divalent sorption sites.

The probability, $p(i,i)$, for two adjacent monovalent counterions $i,i$ to be found on the surface is given by[31,32]

$$p(i,i) = \left[\frac{y(j)}{\sum y(j)}\right]^2 \sum y(j), \quad (23)$$

where $\sum y(j)$ is the sum of the dimensionless loadings of the sorbent with all monovalent counterions. Using the dimensionless loadings $y(i)$, the separation factors (20)–(22) can be expressed as follows:[30,31,36]

$$Q^{H}_{II\,SO_4} = \frac{y(SO_4)[y(H) + y(Cl) + y(Na)]}{[y(HO)]^2[c(H^+)]^2 c(SO_4^{2-})}, \quad (24)$$

$$Q^{H}_{II\,Cl} = \frac{[y(Cl)]^2}{[y(HO)]^2[c(H^+)]^2[c(Cl^-)]^2} \equiv (Q^{H}_{I\,Cl})^2, \quad (25)$$

$$Q^{H}_{II\,Na} = \frac{[y(HO)]^2[c(Na^+)]^2}{[y(Na)]^2[c(H^+)]^2} \equiv (Q^{H}_{I\,Na})^2. \quad (26)$$

Analogous relationships can be derived for those relatively rare cases where trivalent cations (*e.g.*, $Al^{3+}$) are involved in ion exchange processes.

### e. Equilibrium parameters for differently charged counterions

If an ion exchange system contains exclusively monovalent counterions and a sorbent contains divalent sorption sites, the equilibrium parameters $\log K^{H}_{II\,i}$ and $m_{II}(H,i)$ should be transformed to the parameters for monovalent sorption sites $\log K^{H}_{I\,i}$ and $m_I(H,i)$ using the following relationships[30,31,36]

$$\log K^{H}_{I\,i} = \frac{\log K^{H}_{II\,i}}{2}, \quad (27)$$

$$m_I(H,i) = \frac{m_{II}(H,i)}{2}. \quad (28)$$

If an ion exchange system contains a mixture of monovalent and divalent counterions, calculations should be carried out assuming divalent sorption sites. The equilibrium parameters $\log K^{H}_{I\,i}$ and $m_I(H,i)$ derived for systems with monovalent counterions should be replaced by the parameters $\log K^{H}_{II\,i}$ and $m_{II}(H,i)$ converted using relationships (27) and (28).

## 4. Pure cation (anion) exchange on weak electrolyte resins

### a. Weakly acid ion exchangers

The equilibrium of the uptake of, *e.g.*, $Na^+$ cations on weakly acid ion exchangers can be schematically described as follows:

$$\overline{R-COOH} + Na^+ \rightleftharpoons \overline{R-COO^- - Na^+} + H^+, \quad (29)$$

where $\overline{R}$ is the polymeric matrix of the ion exchanger (according to commonly accepted designations, the species under the horizontal line refer to the ion exchanger phase). Normally, weakly

acid ion exchangers cannot adsorb anions. Hence, the terms for anions in the general Eqn (19) of the SCT model vanish. Correspondingly, the equation of the SCT model is simplified [30, 31, 36]

$$\log Q^{H}_{Na} = \log K^{H}_{Na} + m(H, Na)y(Na). \quad (30)$$

**b. Weakly basic ion exchangers**

The uptake of a mixture of cations and anions (*e.g.*, $H^+$ and $Cl^-$) by weakly basic polymeric ion exchangers can be written as

$$\overline{R-NH_2} + H^+ + Cl^- \rightleftharpoons \overline{R-NH_3^+-Cl^-}. \quad (31)$$

Because weakly basic ion exchangers do not sorb alkali metal and alkaline-earth metal cations, Eqn (16) is simplified [30, 31, 36]

$$\log Q^{H}_{Cl} = \log K^{H}_{Cl} - m(H, Cl)y(Cl). \quad (32)$$

The uptake of chloride ions by the protonated functional groups of the ion exchanger is also described as the exchange of $Cl^-$ ions for hydroxy groups [34]

$$\overline{(R-NH_2)\cdot H_2O} + Cl^- \rightleftharpoons \overline{R-NH_3^+-Cl^-} + OH^-. \quad (33)$$

In this case consideration of the ion equilibrium in the framework of the SCT model is performed analogously to that given in Section II.3 and leads to the following relationship

$$\log Q^{OH}_{Cl} = \log K^{OH}_{Cl} + m(OH, Cl)y(Cl). \quad (34)$$

## 5. Strongly acid and strongly basic ion exchangers

The SCT model also allows the relationships for the description of equilibria for sorption of ions by strongly acid and strongly basic resins to be derived from Eqn (19). However, one should keep in mind that in the case of cation exchangers the hydrogen ions cannot be assumed to be adsorbed on the surface, because of complete dissociation of the ion exchanger. Besides, protons are surrounded by the hydration shell and therefore cannot closely approach the surface. Similar considerations also hold for another sorbent–sorbate pair, namely, a strongly basic anion exchanger and $OH^-$ ions. For both strongly acid and strongly basic ion exchangers the sequence of the Stern layers begins with the layer corresponding to that kind of counterions which is located in the closest proximity to the surface.[30, 31, 36]

## 6. Liquid-phase equilibrium relationships

The liquid-phase ion equilibria are calculated using the following equations: relationships for the dissociation of water, mass balances for each component and the condition for electroneutrality. The activity coefficients in the liquid phase can be calculated from the ionic strength of the solution using the Debye–Hückel relationship.[54]

Note that in systems containing water, hydrolysis of trivalent (*e.g.*, $Al^{3+}$) cations should be taken into account. The formation constants of the charged and neutral molecules can be found in the literature (see, *e.g.*, Refs 54–57).

# III. Uptake of ions due to Lewis acid/Lewis base interactions

## 1. Reactions on the sorbent surface

The sorption of chloride ions by weakly basic anion exchangers can be treated as adsorption of the acid by free amino groups [see Eqn (31)]. A similar character of the uptake of cations and an equivalent amount of anions is due to the Lewis-base properties of amino groups, which can be coordinatively bound to Lewis acids (metals, M). Taking chloride and copper ions as examples, the equation for this kind of sorption can be written as follows:[33, 34, 38, 55]

$$\overline{R-NH_2} + Cu^{2+} + 2Cl^- \rightleftharpoons \overline{R-NH_2[Cu^{2+}(Cl^-)_2]}. \quad (35)$$

Metal coordination can occur in a variety of fashions. Figure 2 shows a schematic (in the framework of the SCT model) diagram of the Stern layers for an ion exchange system containing protons, two kinds of divalent metal cation $M_A^{2+}$ and $M_B^{2+}$ and monovalent and divalent anions $X_A^-$ and $X_B^{2-}$.

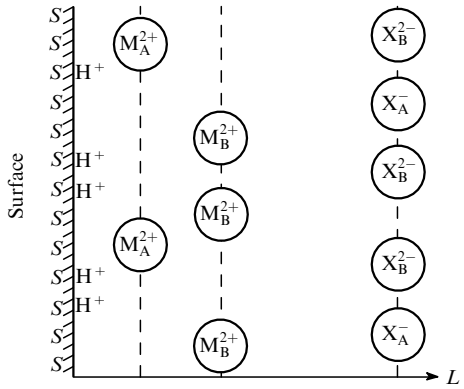



**Figure 2.** Ion layers near the surface of a weakly basic ion exchanger during the uptake of metal salts ($L$ is the distance from the surface).[34]

We will assume that metals are present in the liquid phase exclusively as divalent cations. To derive the equilibrium relationships, let us consider the competitive uptake of metal salts and the corresponding strong acids.[33, 34] First, we will analyse a simple ion exchange system containing one kind of metal and one kind of anion species, namely, protons ($H^+$), metal cations ($M^{2+}$) and monovalent anions ($X^-$). As mentioned above, the surface charge of the ion exchanger equals the least common multiple of the charges of the ions sorbed. In the case under study (divalent metals $M^{2+}$), for the parameter $z_R$ we have $z_R = 2$ (see Ref. 34). The surface reactions can be written as follows:[33, 34]

sorption of strong acids $(HX)_2$ or $H_2X_2$

$$\overline{R-(NH_2)_2} + 2H^+ \rightleftharpoons \overline{R-(NH_3^+)_2}, \quad (36)$$

$$\overline{R-(NH_3^+)_2} + 2X^- \rightleftharpoons \overline{R-(NH_3^+-X^-)_2}, \quad (37)$$

overall

$$\overline{R-(NH_2)_2} + 2H^+ + 2X^- \rightleftharpoons \overline{R-(NH_3^+-X^-)_2}; \quad (38)$$

sorption of metal salts

$$\overline{R-(NH_2)_2} + M^{2+} \rightleftharpoons \overline{R-(NH_2)_2-M^{2+}}, \quad (39)$$

$$\overline{R-(NH_2)_2-M^{2+}} + 2X^- \rightleftharpoons \overline{R-(NH_2)_2-[M^{2+}, (X^-)_2]}, \quad (40)$$

overall

$$\overline{R-(NH_2)_2} + M^{2+} + 2X^- \rightleftharpoons \overline{R-(NH_2)_2-[M^{2+}, (X^-)_2]}. \quad (41)$$

The concentrations of surface complexes $\overline{R-(NH_3^+-X^-)_2}$ and $\overline{R-(NH_2)_2-[M^{2+}, (X^-)_2]}$ (in mg-equiv $g^{-1}$) in the reactions (38) and (41) characterise the loadings of the resin with the acid and metal salt, respectively. Applying the mass action law to processes (38) and (41) and taking into account relationship (14), we get the following relationships for calculations of the formation constants of the complexes

$$K_{H_2X_2} = \frac{y(H)}{y(\overline{R-NH_2})c_{St}(M^{2+})[c_{St}(X^-)]^2}, \quad (42)$$

$$K_{MX_2} = \frac{y(M)}{y(\overline{R-NH_2})c_{St}(M^{2+})[c_{St}(X^-)]^2}, \quad (43)$$

where $y(H)$, $y(M)$ and $y(\overline{R-NH_2})$ are the loadings of the resin with the acid and metal salt and the concentration of neutral functional groups, respectively.

By applying the Boltzmann relationship and using the description of the sequence of electrical double layers as electric capacitors connected in series near the surface in the framework of the SCT model it is possible to derive the expressions relating the generalised separation factors to the loadings of the resin with the metal salt and acid [33, 34]

$$\log Q_{MX_2} = \log K_{MX_2} - \frac{2}{\ln 10}\frac{F^2 q_{max}}{RTA_0C_2}y(X), \quad (44)$$

$$\log Q_{H_2X_2} = \log K_{H_2X_2} - \frac{2}{\ln 10}\frac{F^2 q_{max}}{RTA_0C_1}y(H) - \frac{2}{\ln 10}\frac{F^2 q_{max}}{RTA_0C_2}y(X). \quad (45)$$

Using designation

$$B = \frac{2}{\ln 10}\frac{F^2 q_{max}}{RTA_0},$$

Eqns (44) and (45) can be written in a more compact form

$$\log Q_{MX_2} = \log K_{MX_2} + m_2 y(X), \quad (46)$$

$$\log Q_{H_2X_2} = \log K_{H_2X_2} + m_1 y(H) + m_2 y(X), \quad (47)$$

where

$$m_1 = -\frac{B}{C_1(H,M)}, m_2 = -\frac{B}{C_2(H,M)}. \quad (48)$$

From Eqns (46) and (47) it follows that four parameters ($m_1$, $m_2$ and the formation constants of the complexes $K_{MX_2}$, $K_{H_2X_2}$) are required for the description of equilibria in the system under study.

### 2. Ion exchange systems containing two different metals

Competitive sorption in a system with higher dimension compared to that of the system considered above can be treated in a similar way. For instance, for a ternary system containing two different metal cations, $M_A$ and $M_B$, and one kind of anion, $X^{z(X)}$, we get the system of three equilibrium relationships [33, 34]

$$\log Q_{M_BX_n} = \log K_{M_BX_n} - \frac{B}{C_3}y(X), \quad (49)$$

$$\log Q_{M_AX_n} = \log K_{M_AX_n} + \frac{B}{C_2}\left[y(M_B) - y(X)\right] - \frac{B}{C_3}y(X), \quad (50)$$

$$\log Q_{H_2X_n} = \log K_{H_2X_n} - \frac{B}{C_1}y(H) + \frac{B}{C_2}\left[y(M_B) - y(X)\right] - \frac{B}{C_3}y(X), \quad (51)$$

where

$$m_1 = -\frac{B}{C_1(H,M_A)}, \quad (52a)$$

$$m_2 = \frac{B}{C_2(M_A,M_B)}, \quad (52b)$$

$$m_3 = -\frac{B}{C_3(M_B,X)}. \quad (52c)$$

As a consequence, six equilibrium parameters of the SCT model are needed for the ternary ion exchange system containing two kinds of metal ion, $M_A^{2+}$ and $M_B^{2+}$, and the acid $H^+X^-$. The geometric interpretation of Eqns (44)–(47) is straightforward and evaluation of the binary parameters $\{\log K, m\}$ of the SCT model is simple.[26–31, 33–36] In the text below we will give some illustrative examples.

Note that numerical values of the parameters $\{\log K, m\}$ of the SCT model for the binary (bin) systems remain unchanged for ternary (tern) systems, namely [33, 34]

$$\log K_{tern} = \log K_{bin}, \quad (53)$$

$$m_{1,tern} = m_{1,bin}. \quad (54)$$

The quantity $m_3$ of the ternary system corresponds to $m_2$ in the binary case [33, 34]

$$m_{3,tern} = m_{2,bin}; \quad (55)$$

the parameter $m_2$ of the ternary system $H/M_A/M_B$ is calculated as the difference between the respective $m_1$ values of the binary subsystems $H/M_A$ and $H/M_B$

$$m_{2,tern} = m_{1,bin}(M_A) - m_{1,bin}(M_B). \quad (56)$$

This treatment of the ternary ion exchange system can be extended to multicomponent systems containing $N$ different metal cations ($M_i$, $i = A, \ldots i, \ldots, N$) and one type of anion, $X^{z(X)}$.

## IV. Evaluation of the SCT model parameters from experimental data

Experimental studies of ion exchange equilibria were carried out taking systems containing either cation or anion exchangers [26, 29, 36] as well as systems containing amphoteric ion exchangers (in particular, activated alumina and activated carbon) [30–32, 36] as examples. Adsorption equilibria were studied for the sorption of heavy metal salts by commercially available ion exchangers and by weakly basic anion exchangers.[33, 34] Methods of pre-treatment of these materials and the experimental conditions necessary for obtaining the corresponding equilibrium data have been well documented.[26–36] In particular, experimental studies of equilibria in amphoteric systems were carried out at constant concentrations of counterions in the liquid phase and at constant amounts of alumina or activated carbon in each sample. The sample volume-to-mass ratios were adjusted in such a way that the degree of sorption and the equilibrium concentration were sufficiently high to be measured reliably. The equilibrium state is mainly governed by the pH value of the liquid phase; therefore, this parameter was varied in each series of samples. The experimental conditions have been reported in detail.[29–31]

To investigate the adsorption of heavy metal salts, the ion exchange resin samples were equilibrated with acid–metal salt mixtures of different composition. Systems containing hydrochloric and sulfuric acids were studied.[33, 34] Numerous experimental data for ion exchange systems were processed using the SCT model in order to evaluate the binary parameters $\{\log K_j^i; m(i,j)\}$ (see Refs 26–32, 34–36).

### 1. Calculations of the SCT model parameters using experimental data

#### a. Pure cation or anion exchange

In evaluating the equilibrium parameters of the SCT model the generalised separation factors $Q_i^j$ can be determined using the experimental data (the equilibrium concentrations of counterions and resin loadings). Then, a linear dependence of $\log Q_i^j$ on $y_i$ must be plotted. For binary cation or anion exchange systems the corresponding plots allow sets of binary equilibrium parameters $\{\log K_j^i, m(i,j)\}$ of the SCT model to be determined from the $Y$-intercept and the slope of the straight line, respectively.

Figures 3–8 show a number of examples for different types of polymeric ion exchangers.[26–31, 33–36] In Fig. 3 we present linear dependences for two weakly acid resins. Systematic deviations from linearity were found only at small loadings. This is due to the

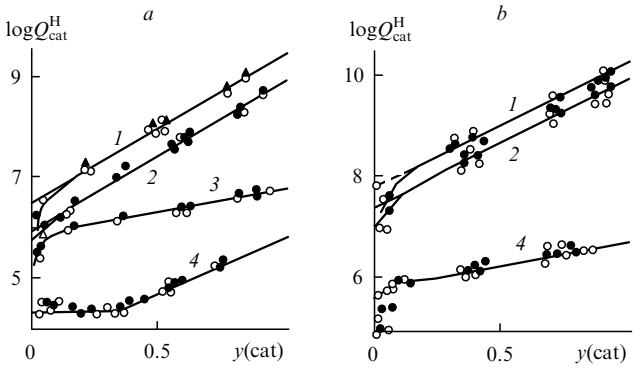



**Figure 3.** Generalised separation factors $Q_{cat}^{H}$ plotted *vs.* loading of sorbent with cations (cat) for the exchange of various divalent cations for protons with two weakly acid ion exchange resins, Lewatit CNP 80 (*a*) and Amberlite IRC 50 (*b*).[31]
Cation: $Mg^{2+}$ (*1*), $Ca^{2+}$ (*2*), $Zn^{2+}$ (*3*) and $Cu^{2+}$ (*4*). Experimental data (full and open circles and full and open triangles) were obtained at different metal salt concentrations in the liquid phase.

fact that basic relationships (19) of the SCT model were derived neglecting low concentrations of counterions in the diffusion layer *D*. They can be included for simple systems (see above), which leads to good agreement between the results of calculations and experimental data for the dependence of $\log Q_i^j$ on $y_i$.[27] Two kinds of sorption sites were discriminated for the sorption of $Cu^{2+}$ counterions by acrylic resin Lewatit CNP 80 (see Fig. 3 *a*): the amount of copper ions adsorbed directly on the surface reaches up to one third of the maximum resin loading, while other $Cu^{2+}$ ions are located far from the resin surface. This is in agreement with the published data on the character of the bonding of $Cu^{2+}$ ions to an acrylic matrix.[57]

Experimental data and the results of SCT calculations of exchange of several anions on a weakly basic ion exchanger are shown in Fig. 4. The visual appearance of the straight lines in the plots indicates that sulfate ions are sorbed at a longer distance from the sorbent surface (larger slope of the corresponding line) compared to chloride and nitrate ions in spite of preferred uptake of the $SO_4^{2-}$ ions by the ion exchanger.

Figure 5 presents the results obtained in evaluating the equilibria with two strongly acid ion exchangers. Exchange of magnesium and sodium counterions and protons for the same

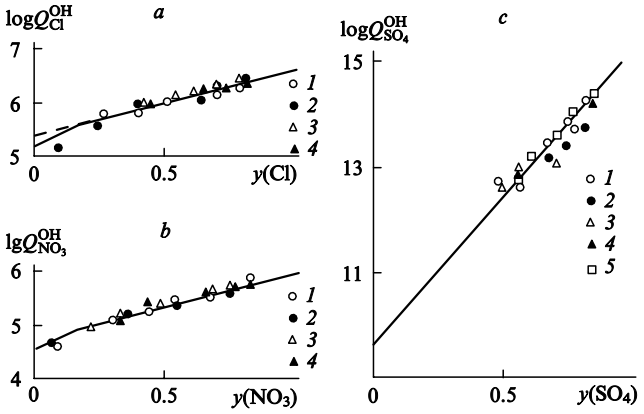



**Figure 4.** Development of generalised separation factors $Q_j^{OH}$ for the exchange of chloride (*a*), nitrate (*b*) and sulfate (*c*) ions (*j*) for hydroxyl ions with the weakly basic ion exchange resin Amberlite IRA 93.[31]
(*a*) *c*(NaCl) /mmol litre$^{-1}$: 0 (*1*), 5 (*2*), 10 (*3*) and 20 (*4*); (*b*) *c*($NaNO_3$) /mmol litre$^{-1}$: 0 (*1*), 5 (*2*), 10 (*3*) and 20 (*4*); (*c*) *c*($Na_2SO_4$) /mmol litre$^{-1}$: 0 (*1*), 5 (*2*), 10 (*3*), 20 (*4*) and 50 (*5*); $c_0$(NaOH) = 10 mmol litre$^{-1}$.

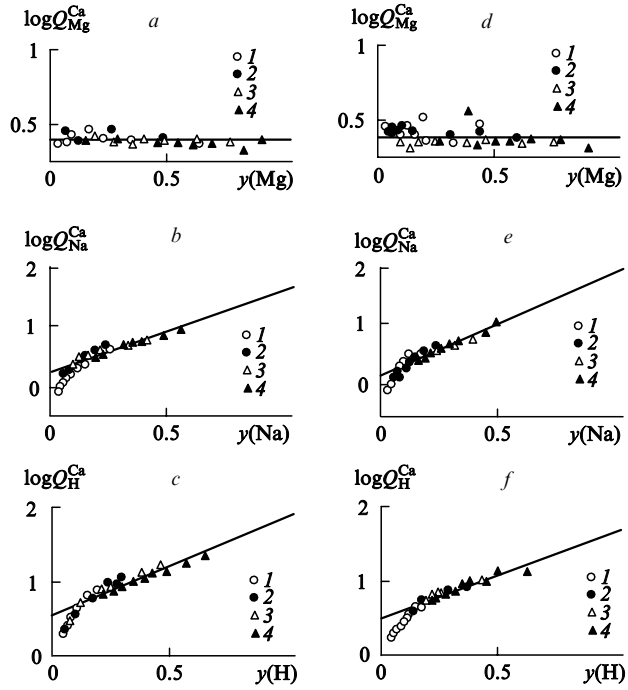



**Figure 5.** Plots of generalised separation factors $Q_{cat}^{Ca}$ for the exchange of magnesium and sodium cations and protons for calcium ions with the strongly acid ion exchange resins Dowex HCRS (*a*–*c*) and Lewatit S 100 (*d*–*f*).[26, 31]
(*a*, *d*) *c*($MgCl_2$) /mmol litre$^{-1}$: 2.5 (*1*), 5 (*2*), 10 (*3*) and 25 (*4*); (*b*, *e*) *c*(NaCl) /mmol litre$^{-1}$: 10 (*1*), 25 (*2*), 50 (*3*) and 100 (*4*);
(*c*, *f*) *c*(HCl) /mmol litre$^{-1}$: 25 (*1*), 50 (*2*), 100 (*3*) and 200 (*4*).

calcium ion used as a reference in the calculations of binary equilibria with other counterions was studied. Similarly to Figs 3

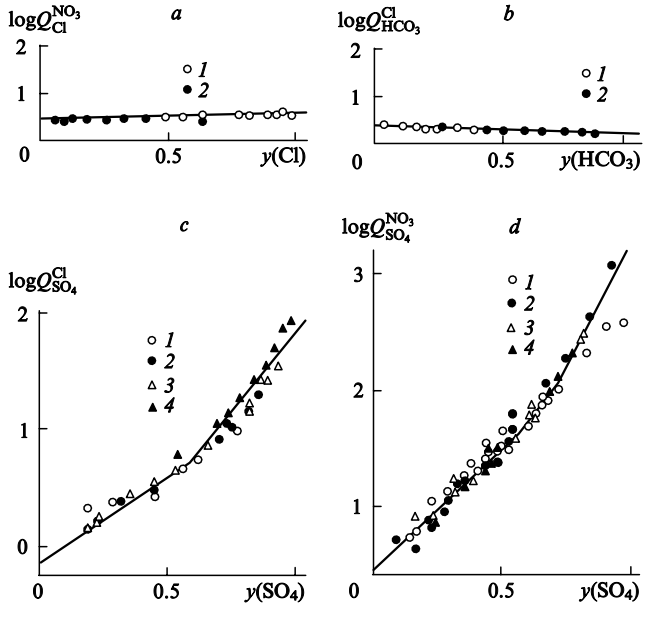



**Figure 6.** Plots of generalised separation factors for different binary exchange equilibria with the strongly basic ion exchange resin Amberlite IRA 410.[26, 31]
(*a*, *b*) *c*($NaNO_3$) /mmol litre$^{-1}$: 5 (*1*) and 50 (*2*); (*c*) *c*($Na_2SO_4$) /mmol litre$^{-1}$: 25 (*1*), 5 (*2*), 10 (*3*) and 50 (*4*); (*d*) *c*($NaNO_3$) /mmol litre$^{-1}$: 5 (*1*), 10 (*2*), 20 (*3*) and 50 (*4*); and *c*($Na_2SO_4$) /mmol litre$^{-1}$: 2.5 (*1*), 5 (*2*), 10 (*3*) and 25 (*4*).

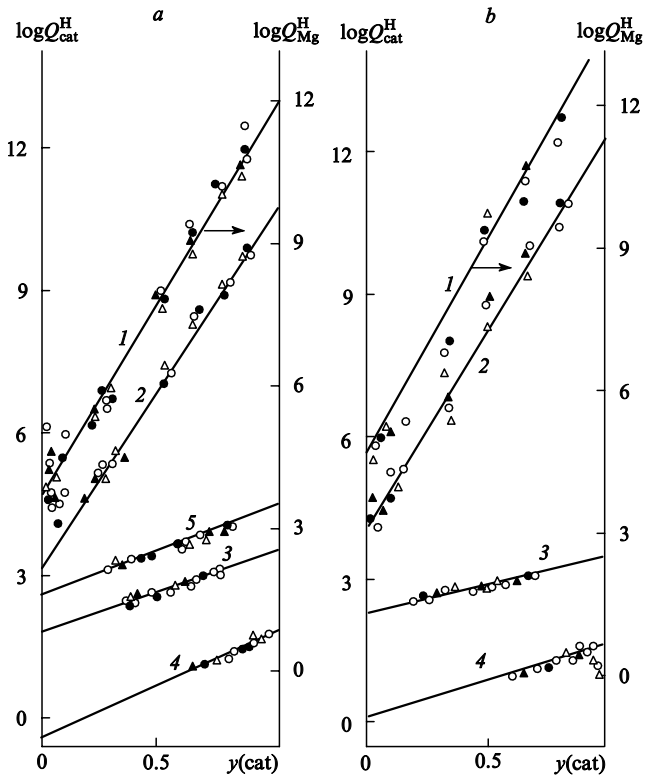



**Figure 7.** Plots of generalised separation factors for $H^+ - Mg^{2+}$ (*1*), $H^+ - Ca^{2+}$ (*2*), $H^+ - Ni^{2+}$ (*3*), $H^+ - Cu^{2+}$ (*4*) and $H^+ - Zn^{2+}$ (*5*) cation exchange with the Lewatit TP 207 (*a*) and Amberlite IRC 718 (*b*) ion exchangers.[26] Experimental data (full and open circles and full and open triangles) were obtained at different metal salt concentrations in the liquid phase.

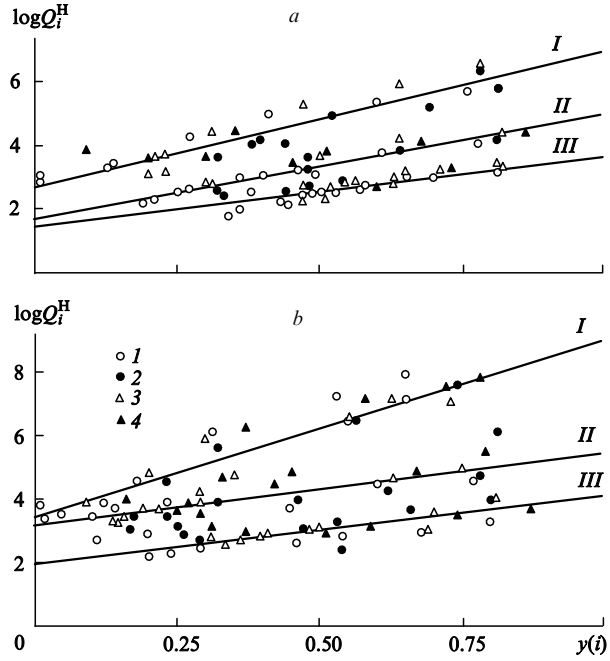



**Figure 8.** Development of generalised separation factors for the exchange of $Ni^{2+}$ (*I*), $Cd^{2+}$ (*II*) and $Cu^{2+}$ (*III*) (*a*) and $Ca^{2+}$ (*I*), $Co^{2+}$ (*II*) and $Zn^{2+}$ (*III*) (*b*) for protons with the Purolite S 940 ion exchanger containing aminophosphonate functional groups (Purolite S 940).[35] $c_0(HCl) = 10$ mmol litre$^{-1}$; $c(MCl_2)$ /mmol litre$^{-1}$: 0 (*1*), 5 (*2*), 10 (*3*) and 25 (*4*); the straight lines were plotted using the linear regression technique.

and 4, the dependences of $\log Q^j_i$ on $y_i$ are approximated by straight lines. However, the regions of deviations from linearity are somewhat larger, which can be due to higher mobility of the counterions in such resins.

Data for anion exchange equilibria on a strongly basic ion exchanger are shown in Fig. 6. As can be seen, the exchange of monovalent anions ($Cl^-/NO_3^-$, $Cl^-/HCO_3^-$) is described by horizontal straight lines. A slightly negative slope was found for the $Cl^-/HCO_3^-$ exchange (see Fig. 6 *b*). The SCT approach treats this as an artifact, which is due to the fact that the ternary ion exchange system contains not only $HCO_3^-$ ions but also $CO_3^{2-}$ species ignored in the binary calculations. The exchange of sulfate ions is characterised by an increase in the slopes of the $\log Q^j_i - y_i$ dependences with an increase in $y(SO_4)$ (kink of the lines in Figs 6 *c*, *d*). Obviously, in this case different near-surface Stern layers are formed, which are successively filled with sulfate ions. This is consistent with the fact that strongly basic anion exchangers contain a variety of functional groups. Again, we can state that divalent sulfate ions are sorbed at longer distances from the surface compared to monovalent counterions (see Figs 6 *c*, *d*).

Evaluation of ion exchange equilibria using the SCT model were successfully extended to the systems containing organic counterions, *e.g.*, oxalate, malate and EDTA species. It was found that the corresponding separation factors $\log Q^j_i$ are linear functions of $y_i$ and the binary parameters $\{\log K^i_j; m(i,j)\}$ of the SCT model were determined (Table 1).

Figure 7 presents the results of calculations of equilibria on two chelating selective resins Lewatit TP 207 and Amberlite IRC 718 containing iminodiacetate groups for the exchange of protons for divalent (calcium, magnesium, copper, zinc and nickel) cations. Analogous dependences obtained in calculations of equilibria on resins containing aminophosphonate functional groups are shown in Fig. 8. In both cases linear dependences of $\log Q^j_i$ on $y_i$ can be deduced. The equilibrium constants $\{\log K^A_B; m(A,B)\}$ calculated using the experimental data for equilibria on different resins are listed in Table 1.

**b. Amphoteric surfaces**

In the framework of the SCT model evaluation of equilibria on amphoteric surfaces requires a more sophisticated procedure compared to those considered above. The first step (prior to calculations) is the assumption of a certain sequence of the Stern layers. Calculations begin with the evaluation of the equilibrium for the exchange of protons at the surface and counterions in the adjacent (first) layer. Calculations of the sorption of ions in the next Stern layer require the corresponding parameters for the first layer. Determination of the SCT model parameters for the third Stern layer requires both sets of binary parameters $\{\log K^A_B; m(A,B)\}$ of the two inner (first and second) layers. The procedure should be continued until all sets of binary parameters for all the Stern layers are calculated. The sequence of the Stern layers is treated as determined correctly if both calculated sets of binary parameters $\{\log K^A_B; m(H,i)\}$ of the SCT model show a monotonic increase in the parameter values with the distance from the surface. If this condition is not met, the computational procedure must be repeated using a modified sequence of Stern layers.

Let us consider a system of Stern layers for $H^+$, $Cl^-$, $NO_3^-$ and $Na^+$ on activated alumina (see Fig. 1) as a simple example. The equilibrium parameters are calculated using the following relationships of the SCT model:[30, 31, 36]

$$\log Q^H_{Cl} = \log K^H_{Cl} + m(H,Cl)[y(Na) - y(Cl) - y(NO_3)], \quad (57)$$

**Table 1**. Parameters of the surface complexation theory for strongly basic resins.[26, 32, 33–35]

| Resin | A/B | $z_R$ | $\log K_B^A$ | $m$(A, B) | Resin | A/B | $z_R$ | $\log K_B^A$ | $m$(A, B) |
|---|---|---|---|---|---|---|---|---|---|
| Amberlite IRA 410 | $Cl^-/HCO_3^-$ | 1 | 0.45 | -0.26 | Amberlite IRC 50 | $H^+/Cu^{2+}$ | −2 | 5.72 | 0.84 |
| | $NO_3^-/HCO_3^-$ | 1 | 0.83 | 0.10 | Amberlite IRA 93 | $OH^-/Cl^-$ | −1 | 5.35 | 1.32 |
| | $NO_3^-/Cl^-$ | 1 | 0.46 | 0.06 | | $OH^-/NO_3^-$ | −1 | 4.65 | 1.32 |
| | $NO_3^-/SO_4^{2-}$ | 2 | 0.47 | 2.62 | | $OH^-/SO_4^{2-}$ | −2 | 9.65 | 5.65 |
| | | | −1.03 [a] | 4.45 [a] | Amberlite IRA 68 | $OH^-/NO_3^-$ | −1 | 3.88 | 0.67 |
| Amberlite IRA 458 | $NO_3^-/Cl^-$ | 1 | 0.42 | 0.00 | Dowex MWA-1 | $OH^-/Cl^-$ | −1 | 5.85 | 0.17 |
| | $Cl^-/SO_4^{2-}$ | 2 | −0.4 | 1.54 | | $OH^-/NO_3^-$ | −1 | 5.40 | 0.17 |
| Amberlite IRA 996 | $NO_3^-/Cl^-$ | 2 | 0.91 | -0.08 | | $OH^-/SO_4^{2-}$ | −2 | 15.85 | 3.95 |
| | $NO_3^-/SO_4^{2-}$ | 2 | 2.6 | 2.98 | Lewatit S 100 | $Ca^{2+}/H^+$ | −2 | 0.55 | 1.35 |
| Amberlite IRA 958 | $Cl^-/CuX^{2-}$ (see [b]) | 2 | −1.66 | 1.46 | | $Ca^{2+}/Na^+$ | −2 | 0.23 | 1.47 |
| | $Cl^-/NiX^{2-}$ (see [b]) | 2 | −1.82 | 1.53 | | $Ca^{2+}/Mg^{2+}$ | −2 | 0.40 | 0 |
| Imac HP 555 | $Cl^-/NO_3^-$ | 2 | 0.61 | 2.24 | Dowex HCRS | $Ca^{2+}/H^+$ | −2 | 0.60 | 1.49 |
| | $Cl^-/NO_2^-$ | 2 | −0.76 | 1.86 | | $Ca^{2+}/Na^+$ | −2 | 0.20 | 1.77 |
| | $Cl^-/SO_4^{2-}$ | 2 | 0.33 | 1.57 | | $Ca^{2+}/Mg^{2+}$ | −2 | 0.42 | 0 |
| | $Cl^-/H_2PO_4^-$ | 2 | −0.85 | 1.85 | Lewatit TP 207 | $H^+/Mg^{2+}$ | −2 | 3.80 | 8.20 |
| | $Cl^-$/Y (see [c]) | 2 | 1.08 | 1.27 | (iminodiacetate | $H^+/Ca^{2+}$ | −2 | 3.15 | 5.55 |
| | $Cl^-$/Z (see [d]) | 2 | 0.79 | 1.48 | groups) | $H^+/Cu^{2+}$ | −2 | −0.30 | 2.05 |
| Wofatit SN 36L | $Cl^-/NO_3^-$ | 2 | 0.40 | 2.51 | | $H^+/Ni^{2+}$ | −2 | 1.80 | 1.80 |
| | $Cl^-/NO_2^-$ | 2 | −0.71 | 2.58 | | $H^+/Zn^{2+}$ | −2 | 2.60 | 1.90 |
| | $Cl^-/SO_4^{2-}$ | 2 | 0.48 | 1.43 | Amberlite IRC 718 | $H^+/Mg^{2+}$ | −2 | 4.70 | 9.65 |
| | $Cl^-/H_2PO_4^-$ | 2 | −0.27 | 1.56 | (iminodiacetate | $H^+/Ca^{2+}$ | −2 | 4.12 | 8.23 |
| | $Cl^-$/Y (see [c]) | 2 | 1.08 | 1.44 | groups) | $H^+/Cu^{2+}$ | −2 | 0.20 | 1.40 |
| | $Cl^-$/Z (see [d]) | 2 | 0.79 | 1.37 | | $H^+/Ni^{2+}$ | −2 | 2.30 | 1.25 |
| Sybron Ionac SR-6 | $Cl^-/NO_3^-$ | 2 | 1.10 | 2.33 | Purolite S 940 | $H^+/Cu^{2+}$ | −2 | 1.44 | 2.15 |
| | $Cl^-/NO_2^-$ | 2 | −0.31 | 2.33 | (aminophosphonate | $H^+/Ni^{2+}$ | −2 | 2.63 | 4.22 |
| | $Cl^-/SO_4^{2-}$ | 2 | 0.45 | 1.40 | groups) | $H^+/Zn^{2+}$ | −2 | 1.96 | 2.02 |
| | $Cl^-/H_2PO_4^-$ | 2 | −0.10 | 1.58 | | $H^+/Cd^{2+}$ | −2 | 1.65 | 3.28 |
| | $Cl^-$/Y (see [c]) | 2 | 0.97 | 1.44 | | $H^+/Co^{2+}$ | −2 | 3.11 | 2.22 |
| | $Cl^-$/Z (see [d]) | 2 | 0.88 | 1.33 | | $H^+/Ca^{2+}$ | −2 | 3.37 | 5.62 |
| Lewatit CNP 80 | $H^+/Na^+$ | −1 | 3.65 | 2.78 | | $H^+/Na^+$ | −1 | 1.34 | 3.71 |
| | $H^+/Mg^{2+}$ | −2 | 6.49 | 2.88 | Purolite S 950 | $H^+/Cu^{2+}$ | −2 | 1.66 | 1.56 |
| | $H^+/Ca^{2+}$ | −2 | 5.95 | 2.88 | (aminophosphonate | $H^+/Ni^{2+}$ | −2 | 3.03 | 3.31 |
| | $H^+/Zn^{2+}$ | −2 | 5.80 | 0.89 | groups) | $H^+/Zn^{2+}$ | −2 | 2.30 | 1.18 |
| | $H^+/Cu^{2+}$ | −2 | 4.35 [e] | 0 | | $H^+/Cd^{2+}$ | −2 | 2.44 | 1.66 |
| | $H^+/Cu^{2+}$ | −2 | 5.00 | 2.13 | | $H^+/Co^{2+}$ | −2 | 2.96 | 2.11 |
| | $H^+/Al^{3+}$ | −6 | 11.32 | 3.95 | | $H^+/Ca^{2+}$ | −2 | 2.81 | 4.81 |
| Amberlite IRC 50 | $H^+/Na^+$ | −1 | 4.38 | 2.38 | | $H^+/Na^+$ | −1 | 1.95 | 3.71 |
| | $H^+/Mg^{2+}$ | −2 | 7.73 | 2.32 | | $H^+/NH_4^+$ | −1 | 1.29 | 5.11 |
| | $H^+/Ca^{2+}$ | −2 | 7.40 | 2.32 | | | | | |

[a] $y(SO_4) > 0.6$. [b] X = EDTA. [c] Y is oxalate ion. [d] Z is malate ion. [e] $y(Cu) > 0.33$.

$$\log Q^H_{NO_3} - m(H, Cl)[-y(Cl)] = \log K^H_{NO_3} + \\ + m(H, NO_3)[y(Na) - y(NO_3)], \quad (58)$$

$$\log Q^H_{Na} - m(H, Cl)[-y(Cl)] - m(H, NO_3)[-y(NO_3)] = \\ = \log K^H_K + m(H, K)y(Na). \quad (59)$$

Evaluation of the equilibrium data on the sorption of $Cl^-$, $NO_3^-$ and $SO_4^{2-}$ ions on the Compalox AN7V 800 alumina and on the uptake of carbonate and sulfate ions and $Na^+$ cations by activated carbon using relationships (57)–(59) has been reported.[26, 30, 31, 36] Although the experimental data obtained for the sorption of sodium ions were not satisfactory, calculations led to linear dependences of $\log Q_i^j$ on $y_i$.

## 2. Sorption of metal salts

The binary SCT parameters $\{\log K_B^A; m(A,B)\}$ characterising the sorption equilibria for metals (M) are calculated using Eqns (46) and (47). The SCT parameters for the sorption of metal salts ($m_1$, $m_2$ and the formation constants of complexes, $K_{MX_2}$ and $K_{H_2X_2}$) can be evaluated from experimental data as follows. The first step involves plotting $\log Q_{MX_2}$ *vs.* the dimensionless loading of the resin with the anions $X^-$, $y_X$. Linear regression (lines in Fig. 9 *a*) gives the parameters $\log K_{MX_2}$ as the *Y*-intercept and $m_2$ as the slope of the regression line. Then, the quantity $(\log Q_{MX_2} - m_2 y_X)$ is plotted *vs.* $y(H^+)$ using the experimental data and the $m_2$ value obtained (full and open circles and full and open triangles in Fig. 9 *b*). Linear regression using Eqn (47) again gives the parameters $K_{H_2X_2}$ and $m_1$ (see the corresponding line in Fig. 9 *b*).[34] The results of calculations for a number of systems for exchange of various metal cations and $Cl^-$ anions with a weakly basic ion exchanger are illustrated in Fig. 9. The binary SCT parameters $\{\log K_B^A; m(A, B)\}$ for the $H^+/M^{2+}/Cl^-$ systems on the Purolite A 109 anion exchanger were calculated [34] using relationships (46) and (47) with consideration of the sorption (see Fig. 2) of two kinds of anions ($Cl^-$ or $SO_4^{2-}$).

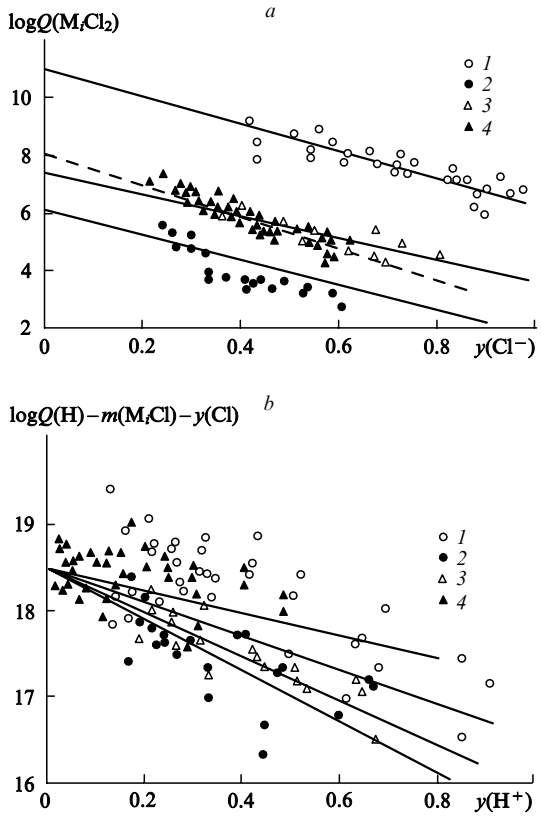



**Figure 9.** Plots of generalised separation factors for the sorption of hydrochloric acid and different metal chlorides ($M_i$) onto the weakly basic ion exchanger Purolite A 109.[34]
The parameter $m_2$ was calculated using Eqn (46) (*a*); the parameter $m_1$ was calculated using Eqn (47). $M_i$: Cu (*1*), Ni (*2*), Cd (*3*) and Zn (*4*).

## V. Calculations of multicomponent equilibria using the SCT model

Calculations of multicomponent ion exchange equilibria in an arbitrary system require a system of conditions to be fulfilled. These are conservation of masses of the components, electroneutrality in the liquid phase and in the ion exchanger phase and chemical equilibria (for, *e.g.*, dissociation or complexation) in the liquid phase.[26–36]

The conditions for electroneutrality (stoichiometry) of exchange describe the constancy of chemical equivalents of components in the liquid phase ($X_s$) and in the resin phase ($y_s$), respectively

$$\sum_{s=\mathrm{A}} X_s = 1, \sum_{s=A} y_s = 1, s = \mathrm{A, B, C, E...}, \tag{60}$$

$$X_s = \frac{z_s c_s}{c_0}, y_s = \frac{a_s}{a_0},$$

where $c_0$ and $a_0$ are the coefficients for conversion of the corresponding concentrations $c_s$ and $a_s$ into dimensionless form.

The major advantage of the SCT approach is that the equilibria in multicomponent ion exchange systems {1, ..., *i*, ..., *j*, ...} can be predicted with ease provided that the binary parameters $\{\log K_j^i;\ m(i,j)\}$ for a number of binary exchanges, *i*/*j*, of the components of the system under study are known. It is particularly convenient if the binary parameters for the exchange of different counterions for the same (reference) counterion are obtained. Consideration of equilibria in a ternary system containing three ions, namely, A (reference), B and C leads to the following relationships:[26]

$$\log Q_{\mathrm{B}}^{\mathrm{A}} = \log K_{\mathrm{B}}^{\mathrm{A}} + m(\mathrm{A,B})[y(\mathrm{B}) + y(\mathrm{C})], \tag{61}$$

$$\log Q_{\mathrm{C}}^{\mathrm{B}} = \log K_{\mathrm{C}}^{\mathrm{B}} + m(\mathrm{B,C})y(\mathrm{C}). \tag{62}$$

As shown above, the equilibrium parameters of the SCT model for the binary exchange A/B in the ternary system A/B/C are the same as in the pure binary case. This also holds for the binary parameters of the A/C exchange. Therefore, only the B/C exchange parameters should be determined, which can be done with ease. The $\log K_{\mathrm{C}}^{\mathrm{B}}$ values are calculated using the relationship[26]

$$\log K_{\mathrm{C}}^{\mathrm{B}} = \log K_{\mathrm{C}}^{\mathrm{A}} - \log K_{\mathrm{B}}^{\mathrm{A}}, \tag{63}$$

while the unknown slope $m$(B,C) in Eqn (62) can be determined using representation of the sequence of Stern layers by electric capacitors connected in series (for substantiation, see above).[26–31] Since the parameter $m(i,j)$ is defined in relationships (18) or (48) *via* the electric capacitance, $C(i,j)$, of the capacitor formed by two Stern layers $(i,j)$, one can make use of the well-known expression for the capacitance ($C$) of two capacitors connected in series (AB and BC)

$$\frac{1}{C(\mathrm{A,C})} = \frac{1}{C(\mathrm{A,B})} + \frac{1}{C(\mathrm{B,C})}. \tag{64}$$

Thus, we get[26, 31, 32, 36]

$$m(\mathrm{B,C}) = m(\mathrm{A,C}) - m(\mathrm{A,B}). \tag{65}$$

Similar relationships were also derived for multicomponent ion exchange systems containing more than three types of counterions.

In Figs 10–12 we present a number of examples of the experimental data and the results of calculations of multicomponent equilibria using the SCT model and corresponding data on binary ion exchange.

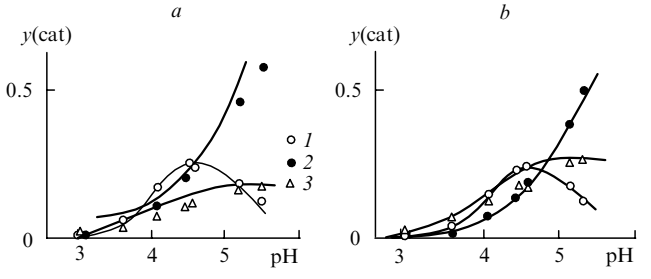



**Figure 10.** Experimental data (full and open circles and open triangles) and the calculated curves of ion exchange equilibria in the quaternary system $Mg^{2+}/Ca^{2+}/Zn^{2+}/H^+$ on the Lewatit CNP 80 weakly acid ion exchanger (originally in the $Ca^{2+}$ form) obtained using the SCT model at $MgCl_2$ concentrations of 25 (*a*) and 50 mol litre$^{-1}$ (*b*), $ZnCl_2$ concentration of 5 mol litre$^{-1}$ and HCl concentration of 10 mol litre$^{-1}$ (see Ref. 26)
$Zn^{2+}$ (*1*), $Ca^{2+}$ (*2*) and $Mg^{2+}$ (*3*).

Figure 10 shows the results obtained for the sorption of different counterions by a weakly acid resin, which originally was in the $Ca^{2+}$ form, in a quaternary ion exchange system. The equilibria are represented as the dimensionless loadings of different cations plotted *vs.* the pH value. As can be seen, the experimental data and the SCT predictions are in good agreement. Similar results were also obtained for strongly acid and strongly basic ion exchangers.[26, 31, 32, 36] In both cases the results of calculations exhibit reasonable agreement with the experimental data.

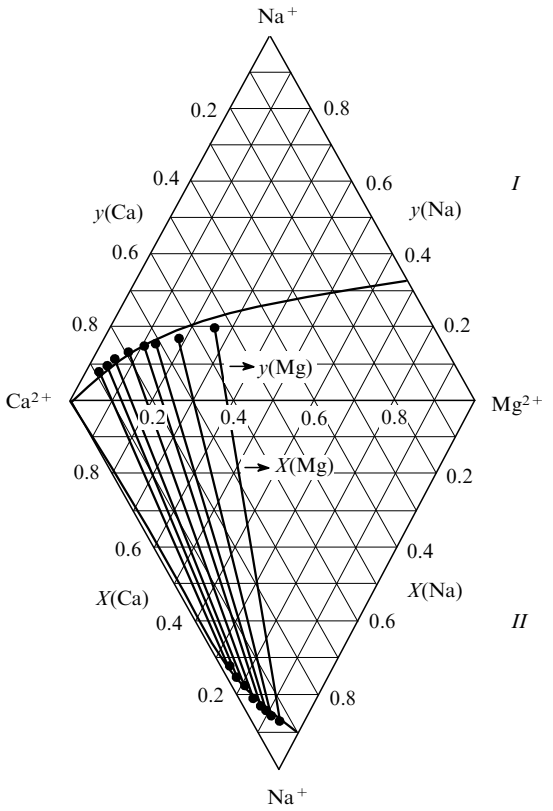



**Figure 11.** Experimental data (full circles) and the calculated curves of ion exchange equilibria in the ternary system $Na^+/Mg^{2+}/Ca^{2+}$ on the Lewatit S 100 strongly acid ion exchanger for the resin phase (*I*) and liquid phase (*II*) obtained using the SCT model.[26]
$y(Na) + y(Ca) + y(Mg) = 1$; $X(Na) + X(Ca) + X(Mg) = 1$; $c_0(Mg) = 2.5$, $c_0(Na) = 50$ mmol litre$^{-1}$.

The exchange of three ions with a strongly acid ion exchanger (Lewatit S 100), which exhibits no preferred affinity towards a particular ion, is illustrated by Fig. 11. Here, we deal with similar concentrations of all components; therefore, the ternary equilibrium can be represented using the triangular diagram. Some differences between the experimental and calculated values for the resin phase can be explained by neglect of the concentration of the counterions in the diffusion layer *D* adjacent to the most distant Stern layer: *N*|*D* (see above).

Figure 12 presents a comparison of the experimental data (full and open circles) with the loadings $y(i)$ calculated using the SCT model for the $NiCl_2/NiSO_4/HCl/H_3BO_3$ and $Ni(SO_3NH_2)_2/HCl/H_3BO_3$ systems on the Purolite S 950 resin containing aminophosphonate functional groups.

The individual equilibrium parameters of amphoteric sorbents were determined above. In Fig. 13 we compare the experimental data on the adsorption equilibria for various counterions (protons, carbonate and chloride ions and calcium cations) on activated carbon. As can be seen, an increase in the pH value of the solution causes the relative loading with chloride ions to decrease and the loadings with calcium, hydrogen and carbonate ions to increase. Nevertheless, the uptake of calcium is small (*i.e.*, the sorbent capacity towards the sorption of these cations is low). Comparison of the results of calculations and experimental data also demonstrates a high predictive power of the SCT model.

The results of an experimental study on the adsorption of $CuCl_2$ and $NiCl_2$ on the Purolite A 109 weakly basic anion exchanger are presented in Fig. 14 as functions of the pH value. These data are in reasonable agreement with the results of calculations using the sets of binary parameters $\{\log K_B^A; m(A,B)\}$ of the SCT model.[26–36]

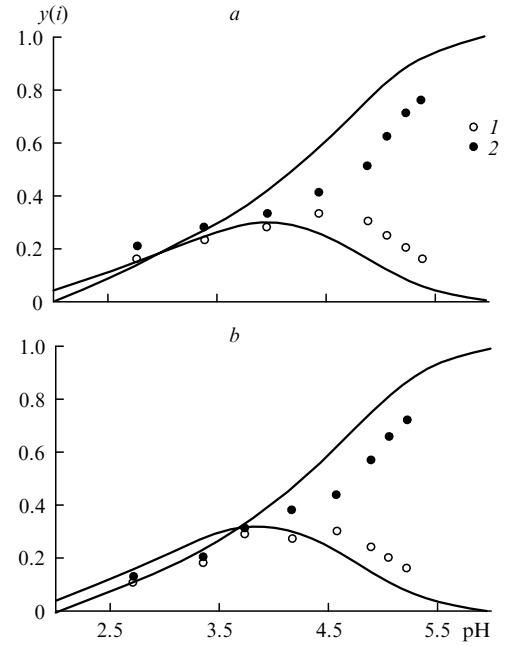



**Figure 12.** Experimental data (full and open circles) and the calculated curves of ion exchange equilibria in the systems $NiCl_2/NiSO_4/HCl/H_3BO_3$ (*a*) and $Ni(SO_3NH_2)_2/HCl/H_3BO_3$ (*b*) on the Purolite S 950 aminophosphonate resin (originally in the $Ca^{2+}$ form) obtained using the SCT model.[35]
(*a*): $c_0(NiCl_2) = 4$, $c_0(NiSO_4) = 6$, $c_0(HCl) = 10$, $c_0(H_3BO_3) = 5$ mmol litre;
(*b*): $c_0(Ni(SO_3NH_2)_2) = 10$, $c_0(HCl) = 10$, $c_0(H_3BO_3) = 5$ mmol litre$^{-1}$; Ni (*1*) and Ca (*2*).

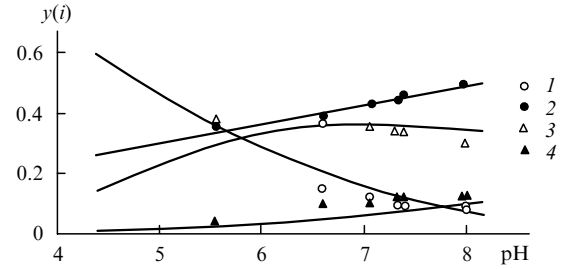



**Figure 13.** Experimental data (full and open circles and full and open triangles) and the predicted loadings of activated carbon (Chemivron F 100) with various species calculated using the SCT model (curves) .[32]
Species: $SOH_2Cl$ (*1*), SOH (*2*), $(SOH_2) = CO_3$ (*3*) and $(SO_2) = Ca$ (*4*).

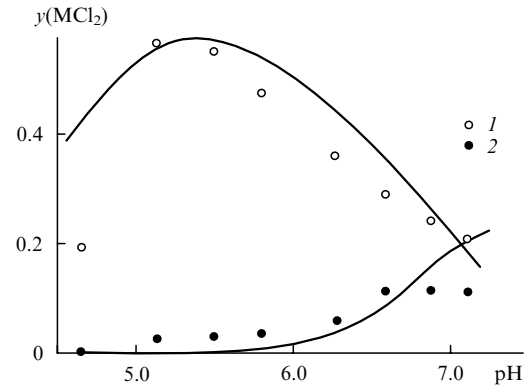



**Figure 14.** Experimental data (full and open circles) and the predicted loadings of the Purolite A 109 anion exchanger with copper chloride (*1*) and nickel chloride (*2*) calculated using the SCT model (curves).[34]
$c_0(CuCl_2) = c_0(HCl) = 5$, $c_0(NiCl_2) = 25$ mmol litre$^{-1}$.

## VI. Application of the SCT model to nonlinear theory of multicomponent sorption dynamics and chromatography

The sorption equilibria characterise the fundamental thermodynamic properties of an ion exchange system.[58–68] The first step in solving problems of multicomponent sorption dynamics is to choose a model for multicomponent equilibria. Until recently the main difficulty consisted in the lack of models suitable for correct description of multicomponent equilibria in real sorption systems. However, in spite of the development of such models, the model of competitive multicomponent sorption proposed by Langmuir remains the most popular as yet. It should be considered as an idealised model, because the separation coefficients, $\alpha_{ij}$, of components in such a nonlinear system of multicomponent equilibria are assumed to be constant and independent of the concentrations $\{X_1,..., X_n\}$ in the mixture of $n$ ions (components).[58–66] In this case the exchange of equally charged ions is described by the following analytical relationships:[58–66]

$$X_i^{eq} = \frac{\alpha_{1i} y_i}{U} = y_i / \sum_{s=1}^{n} \alpha_{is} y_s \,,$$

$$U = \sum_{s=1}^{n} \alpha_{1s} y_s = \alpha_{1n} + \sum_{s=1}^{n-1} (\alpha_{1s} - \alpha_{1n}) y_s,$$

or

$$y_i^{eq} = \frac{\alpha_{i1} X_i}{V} = X_i / \sum_{s=1}^{n} \alpha_{si} X_s \,,$$

$$V = \sum_{s=1}^{n} \alpha_{s1} X_s = \alpha_{n1} + \sum_{s=1}^{n-1} (\alpha_{s1} - \alpha_{n1}) X_s, \qquad (66)$$

$$V = \frac{1}{U}.$$

Here $\alpha$ are the binary separation coefficients, $(s,i)$ or $(i,s)$, of the components in the $n$-component mixture

$$\alpha_{is} = \frac{y_i / X_i}{y_s / X_s},$$

$$\alpha_{is} = \frac{1}{\alpha_{si}}, \; i,s = 1, 2, ..., n, \qquad (67)$$

and $y$ and $X$ are the dimensionless concentrations of ions ($i$ or $s$) in the sorbent phase and in solution, respectively.

The Langmuir model[67] of an idealised localised monolayer was proposed for a one-component system. This simple model is inapplicable to multicomponent mixtures; however, it was formally extended to multicomponent systems.[58–66, 68] Studies on the multicomponent Langmuir model and a number of related phenomenological models were thoroughly reviewed.[58–62, 65, 66] In particular, it was shown[58] that application of the mass action law relationships to the exchange of equally charged ions in a mixture [with consideration of the condition for electroneutrality (60)] allows the sorption equilibria to be formally described by Eqns (66). Analytical relationships (66) and (67) for the description of competitive multicomponent sorption equilibria have long been known.[58–66, 68] The symmetric and simple form of these relationships permits their use in not only numerical solution to problems of the sorption and ion exchange dynamics (for analysis, see Refs 58–66, 69–71) but also electrophoresis theory.[72]

In his review[64] Tondeur analysed theoretical concepts and problems of multicomponent sorption dynamics and chromatography. He pointed out three properties of the Langmuir model which have a significant impact on the modern view of competitive multicomponent sorption dynamics. These are the kinetic approach to the description of equilibria, the symmetric form of relationships (66) and (67) for the Langmuir isotherms and the implications beyond the scope of adsorption theory (see, *e.g.*, Ref. 72).

The basics of the kinetic approach leading to relationships (66) are as follows:[64] (1) an adsorption equilibrium is treated as equality of the sorption–desorption rates simultaneously for all components; (2) the desorption rate of each component is proportional to the relative coverage of the sorbent surface with the corresponding component; and (3) the adsorption rate is proportional to the product of two factors, *viz*., the concentration of a given component in the liquid phase and the fraction of uncovered sorbent surface.

Using relationships (19) and (60), it was shown[26] that the Langmuir competitive model (66) and (67) is naturally described as a particular case for the SCT model provided that two conditions are simultaneously met, namely, all exchanging counterions have equal charges and all SCT parameters $m(i,j)$ are equal to zero. The latter condition means that all the electrical double layers $|i\,j|$ have infinitely large electric capacities [see Eqn (18)]. Therefore, in the framework of the SCT model the Langmuir multicomponent sorption corresponds to the formation of surface complexes of various ions on the same Stern layer (at the surface near the reactive sites).[26] In this case, the generalised separation factors $Q_j^i$ of the SCT model [see Eqn (19)] are transformed into the constants $\alpha_{is}$ [see Eqn (67)] of multicomponent Langmuir isotherms [see Eqn (66)].

The separation factors $\alpha_{ij}$ characterise the relative selectivity of the sorbent in binary exchange $i/j$. Namely, if $\alpha_{ij} > 1$, the component $i$ has a higher affinity than the component $j$. The $i$th concentration distribution ratio

$$\gamma_i = \frac{y_i}{X_i}$$

characterises the affinity towards sorbent of each $i$th component of an $n$-component mixture. Using the concentration distribution ratios, an 'affinity sequence' of the species $(1 > 2 > ... > i > ... > j > ... > n)$ is determined, which is widely used in studies of the dynamics of multicomponent sorption systems. In the 'affinity sequence' the species are arranged in order of decreasing $\gamma$ ($\gamma_i > \gamma_j$). Therefore, the species $i$ (with smaller number in the affinity sequence) possesses a higher affinity towards the sorbent compared to the species $j$, because $\gamma_i > \gamma_j$ (or $\gamma_i/\gamma_j > 1$).

When the mixture composition $\{X_1, ..., X_n\}$ is varied, the position of the components in the 'affinity sequence' may remain unchanged (the so-called 'invariant affinity sequence') or it may vary (this is called 'inversion' or 'selectivity reversal').[51–53, 58, 60, 65] For the Langmuir isotherms (66) inversion is impossible because the separation factors are constants and the affinities of the mixture components remain unchanged. Using Eqns (49)–(51) of the SCT model, the effect of affinity inversion on the shape of multicomponent frontal and displacement chromatograms in the case of ion exchange in the $H^+/M_A^{2+}/M_B^{2+}/An^-$ ($An^-$ is an anion) systems was studied.[51–53]

From the general theory of chromatography it follows that the behaviour of multicomponent concentration waves propagating in a sorption column is mainly governed by the set of adsorption properties of the mixture components which form the corresponding 'affinity sequence'.[51–53, 58–66] Multicomponent sorption equilibria are mainly responsible for the order, shape and velocities of propagation of such waves (examples can be found in the literature[46, 47, 51–53, 58–66]).

The sorption dynamics is described using, *e.g.*, the term 'effect of interference of mixture components' (see a monograph[58] and reviews[63–65]). Generally, the interference of species can arise as a consequence of various forms of their interaction. There are the equilibrium interference effects (mutual influence of species on the equilibrium interphase distributions) and the kinetic interference effects (mutual influence of species on the time taken to establish the equilibrium between the concentrations of a given component in the disperse and continuous phases in the presence of other components). The equilibrium and kinetic interference effects can arise simultaneously upon changes in the state of components

(molecules or ions) due to chemical reactions (*e.g.*, complexation).[58]

Successful solution to a number of problems of sorption dynamics and chromatography related to interference of species and propagation of multicomponent concentration waves became possible after introducing the fundamental coherence concept.[58, 73–76]

The multicomponent model of liquid chromatography is described by a system of nonlinear mass balance equations for each *i*th component of a mixture containing *n* components [58–66, 77]

$$\delta\frac{\alpha_0}{c_0}\frac{\partial y_i}{\partial t}+\frac{\partial X_i}{\partial t}+u\frac{\partial X_i}{\partial Z}=0, \tag{68}$$

$$\frac{\alpha_0}{c_0}\frac{\partial y_i}{\partial t}=\zeta_i[X_i-X_i^{eq}(y_i)], \tag{69a}$$

or

$$\frac{\partial y_i}{\partial t}=\beta_i[y_i^{eq}(X_i)-y_i]. \tag{69b}$$

Here $\delta\equiv(1-\varepsilon)/\varepsilon$ ($\varepsilon$ is the layer porosity); $t$ is time (in s); $u$ is the flow rate of the mobile phase (in m s$^{-1}$); $Z$ is the distance along the sorption layer (in m); and $\zeta_i$ and $\beta_i$ are the kinetic coefficients (in s$^{-1}$) for the film diffusion kinetics and intraparticle diffusion kinetics of limiting stages, respectively.

The mass balance equations (68) and (69) make use of the dimensionless concentrations of the components in the liquid phase ($X_i$) and in the sorbent phase ($y_i$). The equations (69a) or (69b) represent phenomenological model equations of sorption kinetics for mixtures. They are based on the concept of linear driving forces,[78–82] according to which the rate of a kinetic process in the sorbent phase for a given component $i$ is proportional to the corresponding kinetic coefficient $\zeta_i$ or $\beta_i$. In the case under study the effects of longitudinal dispersion are considered insignificant; therefore, the mass balance equation (68) ignores the longitudinal dispersion in the sorption layer of the column.

The system of equations (68) and (69a) [or (69b)] should be augmented with the system of equations for multicomponent sorption isotherms $y_i^{eq}(X)$ [or the system of reverse relationships $X_i^{eq}(y)$], which determines the equilibria between the concentrations of the mixture components in the mobile liquid phase ($X_i$) and in the sorbent phase ($y_i^{eq}$):

$$\begin{aligned} &y_i^{eq}(X)=[X_i^{eq}(y)]^{-1},\\ &y_i^{eq}(X)=y_i^{eq}(X_1, X_2, ..., X_n),\\ &X_i^{eq}(y)=X_i^{eq}(y, y_2, ..., y_n). \end{aligned} \tag{70}$$

To include the relationships of the SCT model of the type (19) for multicomponent ion exchange equilibria in these considerations, one should elaborate relevant computational methods, as well as procedures for solving the dynamic equations (68) and (69). Here, the condition for stoichiometry (equivalence of exchange) [see Eqns (60)] should be taken into account.

The SCT model was employed to describe the dynamics of simple (A/B) binary ion exchange systems in which the concentration fronts of the A/B exchange in the column are considered.[37–39, 43] The shape of the concentration profile, $X_A(Z,t)$, is governed by the shape of the binary isotherm $y^{eq}(X_A)$, which depends on the binary parameters $\{K_B^A; m(A,B)\}$ of the SCT model and on the counterion charge ratio, $z_A/z_B$ (see Refs 26, 36–39, 50). The corresponding relationships of the SCT model for the (A/B) binary ion exchange systems have the form

$$\frac{y_A^{eq}(X_B^{eq}/z_B)^{2/z_B}}{y_B^{eq}(X_A^{eq}/z_A)^{2/z_A}}=K_B^A\exp[\ln 10(m_{AB}y_B^{eq})], \tag{71}$$

where $y_B^{eq}=1-y_A^{eq}$; $X_B^{eq}=1-X_A^{eq}$.

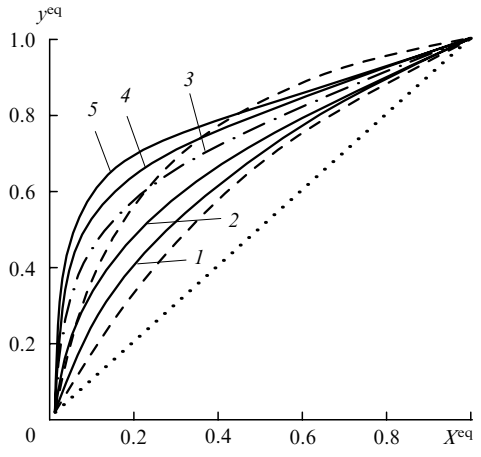



**Figure 15.** Binary A/B ion exchange isotherms at $z_A/z_B = 1$ and $K_B^A = 2$; $m(A,B) = 0.2$ (*1*), 0.5 (*2*), 1.0 (*3*), 1.5 (*4*) and 2 (*5*).[50]
Two Langmuir isotherms [$m(A,B) = 0$; $K_B^A = 2$ and 5] are shown by the dashed lines and the diagonal of the 'concentrational rectangle' is shown by the dotted line.

The binary exchange isotherms calculated at different values of the parameters $\{K_B^A; m(A,B)\}$ and different $z_A/z_B$ ratios are shown in Figs 15 and 16 (see also Ref. 26). As can be seen, their curvatures and asymmetries depend on the joint effects of the two SCT parameters. The curvatures of the isotherms monotonically increase with an increase in the parameters $m(A,B)$ (see Fig. 15) and $K_B^A$ (see Fig. 16). A comparison of the plots for the same values of the SCT parameters at different $z_A/z_B$ ratios (dash-and-dotted curves in Figs 15 and 16) shows that the larger the $z_A/z_B$ ratio, the higher the curvature of the isotherm.

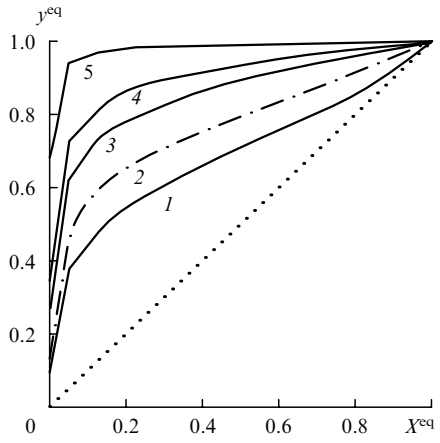



**Figure 16.** Binary A/B ion exchange isotherms at $z_A/z_B = 3/2$ and $m(A,B) = 1$; $K_B^A = 1$ (*1*), 2 (*2*), 5 (*3*), 10 (*4*) and 100 (*5*).[50]
The diagonal of the 'concentrational rectangle' is shown by the dotted line.

The SCT isotherms for equally charged counterions at $m = 0$ (dashed lines in Fig. 15) are reduced to the Langmuir isotherms. In the region of normalised concentrations ($0 < y^{eq}, X^{eq} < 1$), the binary Langmuir isotherms are symmetrical with respect to the back diagonal.[26] At the same time, the binary SCT isotherms for exchange of differently charged counterions ($z_A \neq z_B$) are essentially asymmetric (see, *e.g.*, inflection points in the plots in Fig. 16).

## VII. Steady-state binary concentration distributions

The results of computer simulation were compared with the theoretical results obtained using analytical solutions of the mass balance equations (68) and (69) for binary (A/B) ion exchange and a steady-state concentration front $X_A$ using relationship (71) at different values of the binary parameters $\{K_B^A; m(A,B)\}$.[37–39, 42, 43] This was done (for analytical solutions, including differently charged ions $z_A$, $z_B$ and the case $m = 0$, see Refs 37 and 38) using an original code written for calculations of the dynamics of ion exchange in multicomponent systems. To test the code and evaluate the accuracy of the results obtained, the breakthrough binary output curves were calculated for both intraparticle (see Ref. 38) and film diffusion kinetics [37, 43] in various nonlinear ion exchange systems.

The mass balance equation (69a) for binary exchange of equally charged ions ($z_A = z_B$) was found to be integrable at $0 < m(A,B) < 1$ assuming film diffusion kinetics. The corresponding analytical solutions which describe steady-state concentration waves for A/B binary exchange were first reported recently.[42] In Fig. 17 we compare the results of numerical simulation and the theoretical results obtained using analytical solutions.[42,50] Shown are the output concentration distribution curves for a binary ion exchange system at different HETP values. The parameter HETP characterises the efficiency of the sorption layer in the column. It is related to the kinetic coefficient $\zeta$ (or $\beta$) by a simple algebraic relationship,[82] which in the case of film diffusion kinetics has the form

$$\mathrm{HETP} = \frac{2u(a_0/c_0)^2}{\zeta(1 + \delta a_0/c_0)^2}.$$

From the general theory of chromatography it follows that the higher the curvature of the SCT isotherms the greater the slope of the calculated profiles of the corresponding concentration fronts.[39, 42, 50] Clearly, the smaller the HETP value for the same isotherm the narrower the concentration front (*cf.* curves *1–3* in Fig. 17).

Agreement between the results obtained using analytical solutions and numerical calculations for steady-state concentration fronts in A/B binary exchange systems points, first, to high accuracy of the iterative numerical procedure employed for both ion exchange equilibria and component concentrations in a dynamic sorption process and, second, to successful implementation of the SCT model in computer simulation of the ion exchange dynamics in nonlinear multicomponent systems.

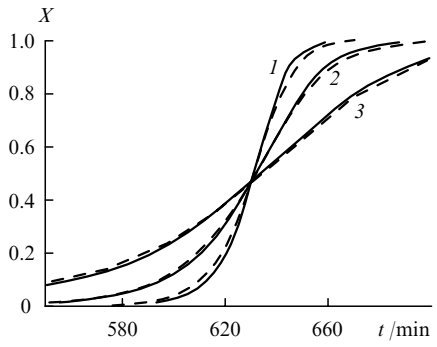



**Figure 17.** Steady-state breakthrough concentration distributions for binary exchange at the SCT model parameters $K_B^A = 2$, $m = 0.12$ and different heights of equivalent theoretical plate (HETP). HETP = 0.5 (*1*), 1 (*2*) and 2 cm (*3*).[42] Solid lines correspond to analytical solutions and dashed lines correspond to the results of numerical calculations; column length is $L = 30$ cm; film diffusion kinetics.

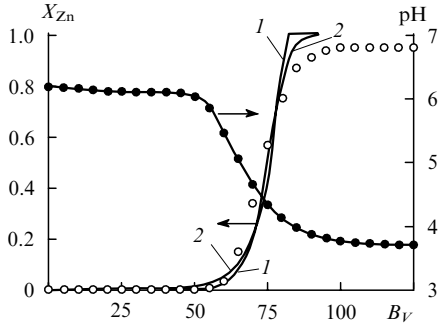



**Figure 18.** Breakthrough concentration dependences for the $Zn^{2+}/Ca^{2+}$ exchange on the Purolite S 940 ion exchanger.[83]
Film diffusion kinetics (*1*) and intraparticle diffusion kinetics (*2*). Full and open circles stand for experimental data while the results of calculations are shown as solid curves; $B_V$ is the number of column volumes.

Summing up, note that Kiefer [83] studied a number of binary systems containing metal ions ($Cu^{2+}/Ca^{2+}$, $Ni^{2+}/Ca^{2+}$, $Zn^{2+}/Ca^{2+}$, $Cd^{2+}/Ca^{2+}$) and compared the calculated and experimental output concentration curves obtained with columns filled with various Purolite resins (S 950, S 940, D 3342, D 3343). As an example in Fig. 18 we present the curves for the $Zn^{2+}/Ca^{2+}$ ion exchange system on the Purolite S 940 resin. As can be seen, the results of numerical calculations are in agreement with experimental data.

## VIII. Computerised description of ion exchange dynamics in multicomponent systems using the SCT model

Nonlinear mass balance equations for multicomponent systems are solved using the method of finite differences and an appropriate explicit numerical computational scheme (predictor–corrector).[84] To calculate various types of multicomponent equilibria based on the SCT model, iterative procedures have been developed.[37–40, 43, 44, 46–53]

Test calculations of multicomponent frontal and displacement chromatograms using an original code have been reported.[37–39, 50] As an example, in Figs 19 and 20 we present such chromatograms for Langmuir-type ion exchange systems [see Eqns (66)] containing equally charged ions (A, B, C, E) that form the 'affinity sequence' A > B > C > E in order of decreasing affinity towards sorbent. The chromatograms in Figs 19 and 20 were obtained for the ternary (A/B/C) and quaternary (A/B/C/E) exchange systems, respectively.

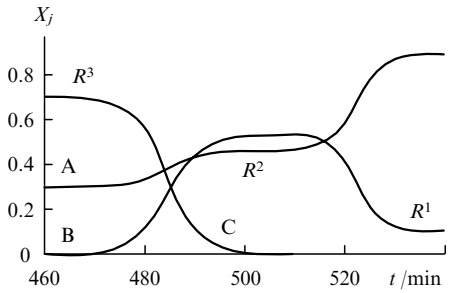



**Figure 19.** Steady-state concentration profiles in the output chromatogram for a ternary exchange system of equally charged ions A/B/C; column length $L = 100$ cm.[38, 39]
Concentration plateau: $R^1$ {0.9; 0.1; 0}, $R^2$ {0.466; 0.533; 0}, $R^3$ {0.3; 0.7; 0}.

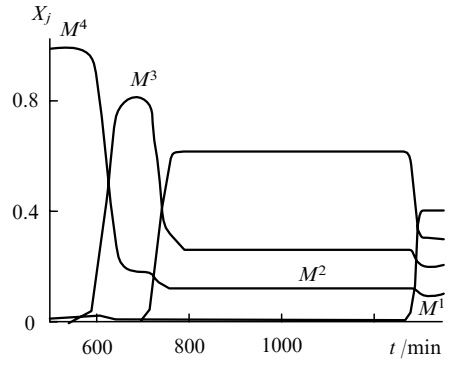



**Figure 20.** Steady-state concentration profiles in the output chromatogram for a quaternary exchange system of equally charged ions A/B/C/E; column length $L = 30$ cm.[38,39]
Concentration plateau: $M^1$ {0.4; 0.3; 0.2; 0.1}, $M^2$ {0; 0.616; 0.264; 0.118}, $M^3$ {0; 0; 0.885; 0.115}, $M^4$ {0; 0; 0; 1}.

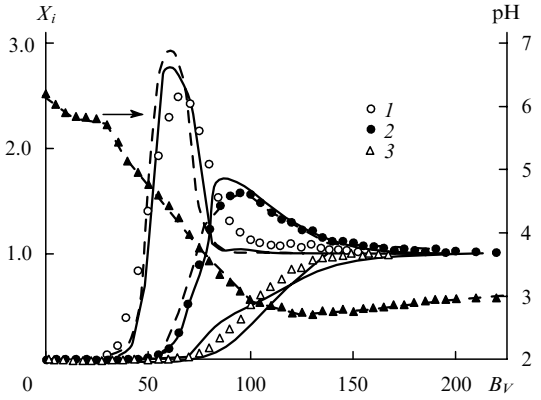



**Figure 21.** Experimental (full and open circles and open triangles) and calculated (curves) chromatograms for the $Cu^{2+}/Ni^{2+}/Zn^{2+}$ exchange on a column with the Purolite S 940 ion exchanger (originally in the $Ca^{2+}$ form).[50,83]
The dashed lines correspond to film diffusion kinetics and the solid lines correspond to intraparticle diffusion kinetics; Ni (*1*), Zn (*2*) and Cu (*3*).

For multicomponent Langmuir systems the concentrations at the plateau $R^s$ (see Fig. 19) or $M^s$ (see Fig. 20) separating the concentration $s$-waves ($s$ is the wave number; $s = 1, 2,...$) were calculated[37–41] analytically using the relations derived for the idealised equilibrium dynamic model (see Refs 58 and 74). In the steady-state regime the concentrations at the plateau on the left ($R^s$ or $M^s$) and on the right ($R^{s+1}$ or $M^{s+1}$) of a concentration $s$-wave depend exclusively on the equilibrium properties of the ion exchange systems and are determined by the parameters of multicomponent Langmuir isotherms [separation factors $\alpha_{ij}$, see Eqn (67)].[58] Both analytical solutions and computer simulation of the dynamic process gave the same values of the concentrations $X_i^{(s)}$ at the multicomponent concentration plateau.

The results of numerical calculations of the concentration profiles shown in Figs 19 and 20 were compared with the results obtained using a number of analytical solutions[63,69–71] for multicomponent Langmuir systems assuming that all components of the mixture are characterised by the same dispersion parameters ($\beta_1 = \beta_2 = ... = \beta_m$ or $\zeta_1 = \zeta_2 = ... = \zeta_m$). Here, it is convenient to use a simple criterion derived from analytical solutions for the Langmuir isotherms.[63,69–71] At equal kinetic dispersion factors of the steady-state waves of the mixture components, relationships between the dimensionless and normalised concentration distributions ($N_i^s$) for each $i$th component of the multicomponent mixture are linear

$$N^s = N_i^s = \frac{X_i - X_i^s}{X_i^{s+1} - X_i^s} = N_j^s = \frac{X_j - X_j^s}{X_j^{s+1} - X_j^s}, \qquad (72)$$

$1 < i, ..., j < m$.

From this it follows that the variable concentration $N^s$ in the multicomponent concentration $s$-wave is the same for all components. Similar linear relationships were obtained[37–39] in computer simulation of the $R^sR^{s+1}$ and $M^sM^{s+1}$ concentration waves (see Figs 19 and 20) in the Langmuir systems, which indicates a high accuracy of numerical calculations.

Column experiments[83] with a number of ternary and quaternary ion exchange systems showed that the corresponding equilibria are well described by the SCT model.[25–36] Multicomponent frontal and displacement chromatograms for the exchange of various metal ions ($Cu^{2+}$, $Ni^{2+}$, $Zn^{2+}$, $Cd^{2+}$, $Ca^{2+}$) were obtained. Experimental studies[83] and numerical calculations[37–39] were carried out for both film diffusion and intraparticle diffusion kinetics. As an example, Fig. 21 shows the experimental chromatographic data obtained for a quaternary exchange system and the corresponding results of numerical calculations. A comparison revealed reasonable agreement between the theory and experiment, especially taking into account the difficulties in obtaining such multicomponent chromatograms and their relative accuracy.

Thus, the above-mentioned method of numerical calculations of the ion exchange dynamics in multicomponent systems and the iterative procedure for calculations of multicomponent equilibria allows the SCT model to be successfully employed in studies of the dynamic behaviour of nonlinear multicomponent ion exchange systems.

## IX. Modelling of the dynamics of ion exchange due to Lewis acid/Lewis base interactions, as applied to multicomponent systems

The approach to modelling of multicomponent ion exchange systems based on the SCT model (see Section VIII) was extended[49,51–53] to calculations of the dynamics of the sorption of metal salts involving coordination bonding due to the Lewis-base properties of amino groups of weak-electrolyte ion exchangers (see Section III). In this case, anions of these metal salts are also sorbed in solution near the surface of the weak-electrolyte ion exchanger. According to the SCT model, the distribution of counterions ($M^{2+}$) and co-ions ($X^-$) near the resin surface is shown in Fig. 2.[33,34]

To model this mechanism of sorption, the system of dynamic equations (68) and (69) must be augmented with the SCT equilibria (49)–(52). The corresponding SCT equilibria are calculated iteratively and the equilibrium ion concentrations ($y_i^{eq}$; $X_i^{eq}$) thus obtained are included in the computational scheme for the concentration distributions in the concentration wave moving through the column.[49,51–53]

Two examples illustrating the results of computer simulation of frontal and displacement chromatograms for the $H^+/M_A^{2+}/M_B^{2+}/An^-$ ($An^- = Cl^-$, $SO_4^{2-}$) ion exchange systems[43,49,51–53] are shown in Fig. 22. Since in this system the $H^+/M_A^{2+}/M_B^{2+}/An^-$ ion exchange due to the Lewis acid/Lewis base interaction is accompanied by sorption of metal salt anions, the conditions for electroneutrality in solution and in the sorbent phase have the form:[49,51–53]

$$X_{An^-} = X_A + X_B + X_H, \qquad (73a)$$

$$y_{An^-} = y_A + y_B + y_H. \qquad (73b)$$

Ion exchange systems for exchange of various metals ($Cu^{2+}$, $Ni^{2+}$, $Zn^{2+}$, $Cd^{2+}$) accompanied by sorption of various anions,

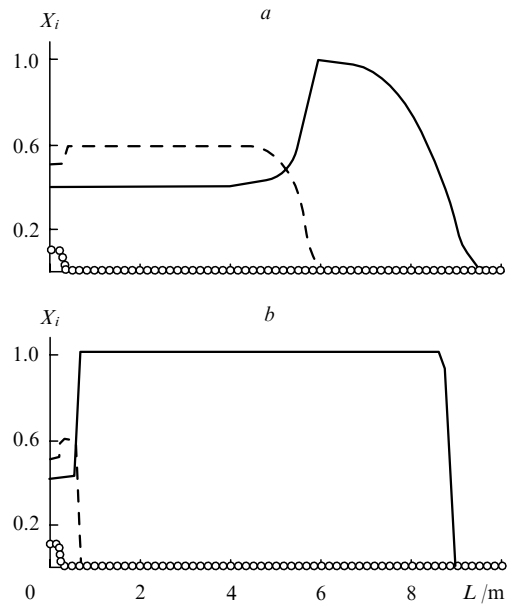



**Figure 22.** Calculated concentration ($X_i$) distributions along a chromatographic column filled with the Purolite A 109 weakly basic anion exchanger for the $H^+/Cu^{2+}/Ni^{2+}/An^{-1}$ exchange accompanied by sorption of $Cl^-$ (*a*) and $SO_4^{2-}$ anions (*b*).[51]
$H^+$ (open circles), $Cu^{2+}$ (dashed lines) and $Ni^{2+}$ (solid lines);
$c_0 = 0.3$ mol litre$^{-1}$, $X^0_H = 0.1$, $X^0_{Cu} = 0.5$, $X^0_{Ni} = 0.4$; $B_V = 7.4\,(a), 2\,(b)$.

namely, chloride ions ($Cl^-$, see Fig. 22 *a*) or sulfate ions ($SO_4^{2-}$, see Fig. 22 *b*) were studied.[49, 51–53] The anion distribution was calculated using Eqn (73a). Dynamic calculations were carried out using the experimental[33, 34] values of the binary SCT parameters $\{K^A_B; m(A,B)\}$.

The total concentration $c_0$ (in mol litre$^{-1}$) of the components, metal salt ions and protons at the column input was kept constant

$$z_A c^0_A + z_B c^0_B + z_H c^0_H = c_0$$

or in the dimensionless form

$$X^0_A + X^0_B + X^0_H = 1.$$

A dimensionless parameter commonly accepted in chromatography (see Fig. 22)

$$B_V = \frac{V_t}{V_0} = \frac{ut}{L}$$

denotes the number of the column volumes, $V_0$, which passed through the cross section of the column of length $L$, and characterises the elapsed time $t$ from the start of the process. The $B_V$ values (see Fig. 22) indicate that the dynamic displacement of metal ions accompanied by the sorption of $Cl^-$ anion is more than three times slower than an analogous process accompanied by the sorption of $SO_4^{2-}$ anions. Indeed, Figs 22 *a* and 22 *b* show that displacement of metal ions (both $Ni^{2+}$ and $Cu^{2+}$) is much more efficient in the presence of divalent $SO_4^{2-}$ anions compared to monovalent $Cl^-$ anions. The influence of the inversion effects on the dynamic behaviour of various related systems for two types of weakly basic anion exchangers has been considered.[51–53]

## X. Dynamics of ion exchange in multicomponent systems with allowance for ion complexation in the mobile liquid phase

Using the SCT model, relationships describing chemical reactions in the liquid phase can be included in calculations of multicomponent equilibria in a relatively simple way.[26, 32] However, in this case the theory of chromatography requires that the nonlinear multicomponent system of dynamic mass balance equations be transformed and represented in the form:[44, 46, 47, 50]

$$\delta \frac{\alpha_0}{c_0} \frac{\partial y_i}{\partial t} + \frac{\partial X_{\text{sum}\,i}}{\partial t} + u \frac{\partial X_{\text{sum}\,i}}{\partial Z} = 0,\ i = 1, 2, \ldots . \tag{74}$$

Now the total concentration of each component, $X_{\text{sum}\,i}$, includes not only the concentration of the ion $i$ in the liquid phase but also the corresponding fractions of this component in various compounds formed as a result of chemical reactions. This approach to simulation of the dynamics of various ion exchange systems with allowance for chemical reactions was employed[44–50] in calculations of the dynamics of the $H^+/M^{2+}_A/M^{2+}_B$ ion exchange with inclusion of complexation reactions.

Let us calculate various ion concentrations taking the $H^+/M^{2+}_A/M^{2+}_B$ exchange with inclusion of complexation reactions in the mobile (liquid) phase of a chromatographic column as an example. Multicomponent equilibria in these systems are described by the SCT model (see Section II) while the accompanying complexation reactions in the mobile (liquid) phase of the column are described by relationships related to the mass action law.

For instance, the ion exchange $H^+/Ni^{2+}/Co^{2+}$ ('affinity sequence' H > Ni > Co) in the presence of citrate ion ($Cit^{3-}$) as a complex-forming agent can be calculated using the following system of relationships:[44, 46, 47, 50]

$$\begin{aligned}
&K_1 = X_1X_4, && K_2 = X_1X_7/X_6,\\
&K_3 = X_1X_8/X_7, && K_4 = X_1X_5/X_8,\\
&K_5 = X_3X_5/X_{14}, && K_6 = X_2X_5/X_9,\\
&K_7 = X_2X_5^2/X_{10}, && K_8 = X_2X_8/X_{11},\\
&K_9 = X_2X_7/X_{12}, && K_{10} = X_5X_{11}/X_{13},\\
&K_{11} = X_3X_8/X_{15}, && K_{12} = X_3X_7/X_{16}.
\end{aligned} \tag{75}$$

Here the constant parameters are $K_1 = 10^{-14}$ [the dissociation constant of water, in (mol litre$^{-1}$)$^2$] and the reaction constants $K_2 - K_{12}$ listed in Table 2; $X_i$ are the dimensionless concentrations of the ions ($i = 1-3$) and the components formed as a result of chemical reactions ($i = 6-16$):

| $i$ | Species | $i$ | Species |
|---|---|---|---|
| 1 | $H^+$ | 9 | $NiCit^-$ |
| 2 | $Ni^{2+}$ | 10 | $NiCit_2^{4-}$ |
| 3 | $Co^{2+}$ | 11 | $NiHCit$ |
| 4 | $OH^-$ | 12 | $NiH_2Cit^+$ |
| 5 | $Cit^{3-}$ | 13 | $NiHCit_2^{3-}$ |
| 6 | $H_3Cit$ | 14 | $CoCit^-$ |
| 7 | $H_2Cit^-$ | 15 | $CoHCit$ |
| 8 | $HCit^{2-}$ | 16 | $CoH_2Cit^+$ |

In accordance with the mass conservation law we have

$$X_0(\text{Cit}) = X_5 + X_6 + X_7 + X_8 + X_9 + 2X_{10} + X_{11} + X_{12} + 2X_{13} + X_{14} + X_{15} + X_{16}. \tag{76}$$

This equality describes the constancy of the total amount of the complex-forming agent ($Cit^{3-}$) in solution.

As usual, in describing the ion exchange we have to take into account the relations of equivalence for the concentrations of free ions ($H^+/Ni^{2+}/Co^{2+}$) in the ion exchanger and in solution:

$$y_1 + y_2 + y_3 = 1, \tag{77a}$$

$$X_1 + X_2 + X_3 = 1. \tag{77b}$$

**Table 2**. Parameters for calculations of ion exchange dynamics in multicomponent systems with inclusion of exchange equilibria described in the framework of the SCT model and complexation reactions.[46, 47, 50]

| System No. | Purolite resin | Ion exchange | Complex-forming agents | Reaction constants [a] | Binary SCT parameters | |
|---|---|---|---|---|---|---|
| | | | | | $\log K_j^H$ | $m(H,j)$ |
| 1 | S 950 | $H^+/Ni^{2+}/Ca^{2+}$ | $H_2BO_3^-$, $SO_3NH_2^-$, $Cl^-$ | $K_1-K_{12}$ | 3.03 | 3.31 |
| | | | | | 2.81 | 4.81 |
| 2 | S 950 | $H^+/Ni^{2+}/Ca^{2+}$ | $H_2BO_3^-$, $SO_4^{2-}$, $Cl^-$ | $K_1-K_{12}$ | 3.03 | 3.31 |
| | | | | | 2.81 | 4.81 |
| 3 | S 940 | $H^+/Cu^{2+}/Ca^{2+}$ | $SO_4^{2-}$ | $K_1-K_4$ | 1.44 | 2.15 |
| | | | | | 3.37 | 5.62 |
| 4 | S 940 | $H^+/Cd^{2+}/Ca^{2+}$ | $NH_3$, $NO_3^-$ | $K_1-K_{12}$ | 1.65 | 3.28 |
| | | | | | 3.37 | 5.62 |
| 5 | S 940 | $H^+/Zn^{2+}/Ca^{2+}$ | $NH_3$, $Cl^-$ | $K_1-K_{12}$ | 1.96 | 2.02 |
| | | | | | 3.37 | 5.62 |
| 6 | S 950 | $H^+/Ni^{2+}/Zn^{2+}$ | $Cit^{3-}$ | $K_1-K_{12}$ | 3.03 | 3.31 |
| | | | | | 2.3 | 1.18 |
| 7 | S 950 | $H^+/Ni^{2+}/Na^+$ | $Cit^{3-}$ | $K_1-K_{10}$ | 3.03 | 3.31 |
| | | | | | 1.95 | 1.82 |
| 8 | S 940 | $H^+/Co^{2+}/Na^+$ | $Cit^{3-}$ | $K_1-K_8$ | 3.11 | 2.22 |
| | | | | | 1.34 | 3.71 |
| 9 | S 940 | $H^+/Zn^{2+}/Co^{2+}$ | $Cit^{3-}$ | $K_1-K_{11}$ | 1.96 | 2.02 |
| | | | | | 3.11 | 2.22 |
| 10 | S 950 | $H^+/Ni^{2+}/Co^{2+}$ | $Cit^{3-}$ | $K_1-K_{12}$ | 3.03 | 3.31 |
| | | | | | 2.96 | 2.11 |

[a] $K_2 = 102$, $K_3 = 4.4$, $K_4 = 6.3 \times 10^6$, $K_5 = 6.2$, $K_6 = 1.26$, $K_7 = 1.66$, $K_8 = 50.1$, $K_9 = 4 \times 10^{-3}$, $K_{10} = 0.008$, $K_{11} = 831$.

In this case the number of the differential mass balance equations (74) for the concentrations $X_{sum\,1}(H^+)$, $X_{sum\,2}(Ni^{2+})$ and $X_{sum\,3}(Co^{2+})$ equals three ($n = 3$):

$$X_{sum\,1}(H^+) = X_1 - X_4 + 3X_6 + 2X_7 + X_8 + X_{11} + 2X_{12} + X_{13} + X_{15} + 2X_{16}, \quad (78a)$$

$$X_{sum\,2}(Ni^{2+}) = X_2 + X_9 + X_{10} + X_{11} + X_{12} + X_{13}, \quad (78b)$$

$$X_{sum\,3}(Co^{2+}) = X_3 + X_{14} + X_{15} + X_{16}. \quad (78c)$$

Numerical simulation of the dynamics of such ion exchange systems was carried out using the experimental[83] values of the binary SCT parameters $\{K_B^A; m(A,B)\}$ obtained for various Purolite resins. The corresponding parameters of the Purolite S 940 and S 950 resins are listed in Table 2. The complexation constants $K_i$ included in relationships (75) can be found in the literature (see, *e.g.*, Ref. 54). To illustrate the large differences between the values of these constants (orders of magnitude), the corresponding data are listed in Table 2.

The nonlinear multicomponent system of dynamic mass balance equations (74)–(78) was numerically solved by the method of finite differences. In this case, in addition to the numerical schemes based on the SCT equilibria (19), iterative procedures for solving the Eqns (75) and (76) describing the complexation reactions with allowance for the relations of equivalence (77) must be included. A software package for calculations of the dynamics of various multicomponent ion exchange systems including quinary systems has been created.[44–48, 50] Some examples are given in Table 2.

Based on the models elaborated, the propagation of $n$-component concentration waves formed in the sorption field of the column was calculated. A number of calculated output frontal-displacement curves for the ion exchange sorption and regeneration in two ion exchange systems are presented in Figs 23 and 24 as examples. Here, shown are the distributions for the exchange of metal ions ($A^{2+}/B^{2+}$); the concentration of the third exchanging ion ($H^+$) is low and the corresponding curves are therefore omitted.

The multicomponent output frontal and displacement chromatograms presented in Fig. 23 in the pseudo-3D space $\{X_i, t, s\}$ are the same as those given in two dimensions in Fig. 24 *c*. The distributions in Fig. 23 clearly illustrate the relative positions of the output concentration curves during the sorption and regeneration processes, obtained for columns of different length $L_s$. The $s$ values ($s = 1, 2, 3, 4$) for columns of different length $L_{1,2,3,4}$ ($L_s$/HETP = 30 or 60) are plotted on the $y$ axis directed 'perpendicular' to the plane of Fig. 23.

In Fig. 24 *a*, *b* we present the calculated output concentration curves obtained for the ion exchange systems Nos 1 and 8 (see Table 2) with allowance for the effect of chemical reactions.[44–48, 50] To compare the dynamic behaviour of different

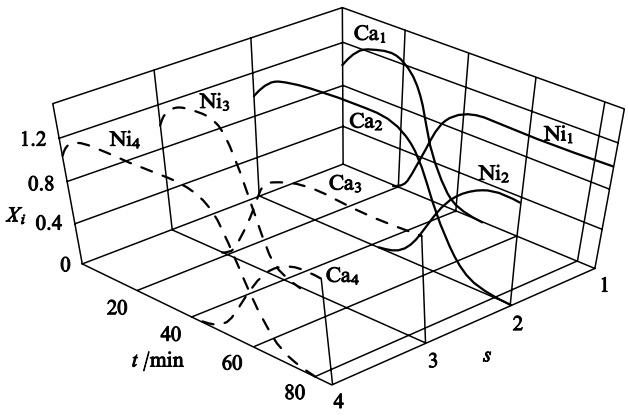



**Figure 23.** Output concentration distributions $X_i(t)$ shown in the $\{X_i, t, s\}$ space for $H^+/Ni^{2+}/Ca^{2+}$ exchange; column lengths are $L_{1,3} = 30$ HETP and $L_{2,4} = 60$ HETP.[46, 50]
$Ni_{1,2}/Ca_{1,2}$ sorption (solid lines), $L_{1,2}$; $Ca_{3,4}/Ni_{3,4}$ regeneration (dashed lines), $L_{3,4}$.

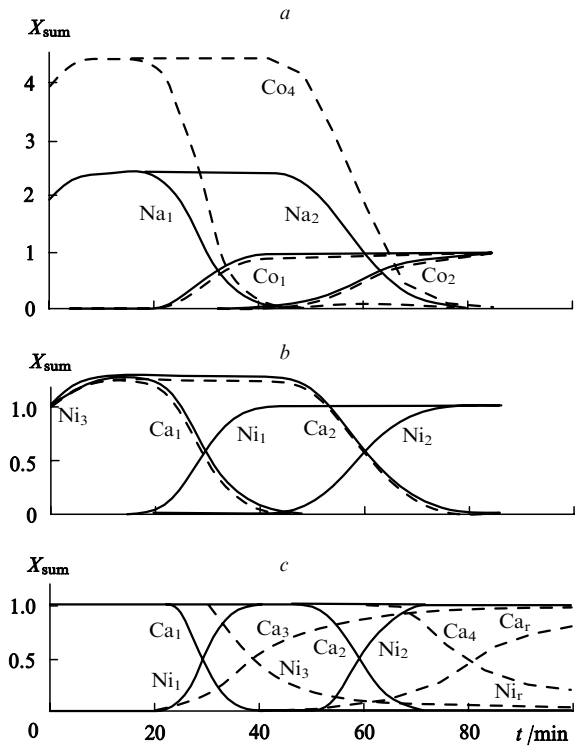



**Figure 24.** Calculated concentration distributions for $H^+/A^{2+}/B^{2+}$ ion exchange on columns of different length $L_s$.[46,47]
$H^+/Co^{2+}/Na^+$ exchange with inclusion of chemical reactions (*a*); $H^+/Ni^{2+}/Ca^{2+}$ exchange with inclusion of chemical reactions (*b*); and $H^+/Ni^{2+}/Ca^{2+}$ exchange ignoring chemical reactions (*c*); solid lines describe the ion exchange (B/A) sorption of the mixture, $X_i(t)$; dashed lines describe the ion exchange regeneration (A/B) of the column, $X_{ir}(t)$ ($Ca_r$, $Ni_r$).

ion exchange systems, Fig. 24 *c* also shows the calculated output curves obtained for the former system in the absence of complexation reactions.

A comparison reveals essential changes in the character of the output concentration curves for the same system caused by the effect of complexation reaction. The output curves of both sorption and regeneration processes obtained with inclusion of complexation exhibit no long 'tails' (see Fig. 24 *a*, *b*); the shapes of the output curves in Fig. 24 *b* obey an identical pattern and the corresponding solid and dashed lines nearly match one another.

In the case of conventional ion exchange the regeneration processes are characterised by the output concentration curves with very long 'tails' (see Fig. 24 *c*), which significantly slow down the regeneration. Besides, both sorption and regeneration accompanied by complexation proceed at higher rates and the output concentrations of the displaced ions are much higher. Therefore, the allowance for chemical reactions permits a more efficient regeneration of ion exchange columns.

## XI. Conclusion

The surface complexation theory used for calculations of multicomponent equilibria has been developed during the last decade.[25–36] It is based on a relatively simple model for the arrangement of ions, which are assumed to be located in ordered Stern layers extended parallel to the planar sorbent surface.

The description of arbitrary equilibria in the framework of the SCT model is based on the concept of generalised separation factors, which can be determined using experimental data on binary exchange. The dependence of these coefficients on the sorbent composition provides valuable information on the binary equilibria. An individual sorption equilibrium can be characterised by two constant parameters of the SCT model, $\{K_{i+1}, m(i,i+1)\}$, which are independent of the pH value or the ionic strength of the solution (liquid phase).[26,30,31,36] These parameters also remain constant in arbitrary multicomponent systems for which simple (binary) equilibria can be calculated for a wide range of experimental conditions.[26–36] The SCT model treats multicomponent equilibria as a kind of superposition of several simple equilibria and allows them to be calculated using the parameters of binary subsystems.[26–36] Arbitrary chemical equilibria in the liquid phase with inclusion of dissociation, association or complexation phenomena can be taken into account in a relatively simple manner for both multicomponent equilibria [30,31,36] and dynamic systems.[44–48,50]

One field of application of the SCT model is the prediction of multicomponent ion exchange kinetics. The potentialities of the approach were demonstrated in calculations of the film diffusion kinetics where this method for the description of equilibria was implemented in solving the Nernst–Planck equations.[85,86]

Sorption equilibria in ternary and quaternary systems with strong- and weak-electrolyte ion exchangers can be predicted very accurately even with inclusion of chemical reactions. The method was incorporated into commercially available software for the design of demineralisers in ultrapure water production.[87]

The theory of formation of surface complexes (or the surface complexation theory, SCT model) can be applied with ease to calculations of the performance of sorption filters. It has been implemented in simple approximate equilibrium calculations using an idealised model in which the filter is represented by a series of stirred tanks (layer-by-layer calculation technique). This approach was shown [88] to be suitable for quite correct prediction of, *e.g.*, combined softening and dealkalisation of water with weakly acid ion exchangers.

The SCT model has also been incorporated into more sophisticated procedures for calculations of dynamic systems based on the theory of multicomponent sorption dynamics and chromatography. This field of application of the SCT approach seems to be quite promising because no appropriate models for multicomponent equilibria suitable for the description of the properties of real sorbents (ion exchangers) were proposed until recently.[37–53]

In a particular case where the SCT parameters $m(i,i+1)$ of all binary exchanges equal zero, the SCT equilibrium relationships are reduced to the well-known multicomponent Langmuir isotherms. This allows the accuracy and correctness of the methods elaborated for solving problems of multicomponent sorption dynamics to be evaluated.[37–42]

Currently, evaluation of the dynamic behaviour of nonlinear multicomponent ion exchange systems is based on the results of calculations of the output column concentration distributions for various ion exchangers.[37–53] Newly developed iterative procedures for calculations of multicomponent equilibria and new software permit successful implementation of the SCT model in the computational schemes for calculations of the dynamic behaviour of nonlinear multicomponent ion exchange systems.

In spite of obvious simplifications of the SCT model, the results obtained demonstrate the efficiency of this method in the calculations of multispecies equilibria and the kinetics and dynamics of sorption in multicomponent systems. The SCT approach can be used in both basic research and applied (in particular, engineering) studies.

Calculations of the propagation of multicomponent concentration waves in the sorption fields of ion exchange columns involve computer simulation. To facilitate perception of the complex dynamics of ion exchange, a kind of computer visualisation is used, namely, animation of the dynamic processes occurring in the chromatographic column.[48–53]

The results presented in this review have been obtained with financial support from the Deutsche Forschungsgemeinschaft (DFG, joint German–Russian Project Nos 463 RUS 113/596/0-1 (R) and 436 RUS 113/83), Deutsche Akademische Aus-

TauschDienst (DAAD, Project No. 325 sm) and the NATO Foundation (Project No. SA 12-2-02, CRG.971709).

## References


1. W Stumm *Chemistry of the Solid— Water Interface* (New York: Wiley, 1992)
2. H V Helmholtz *Wiss. Abh. Phys. Techn.* **1** 925 (1879)
3. C Gouy *J. Phys.* **9** 457 (1910)
4. D I Chapman *Philos. Mag.* **25** 45 (1913)
5. O Stern *Z. Elektrochem.* **30** 508 (1924)
6. R O James, T W Healy *J. Colloid Interface Sci.* **40** 42 (1972)
7. R O James, T W Healy *J. Colloid Interface Sci.* **40** 53 (1972)
8. R O James, T W Healy *J. Colloid Interface Sci.* **40** 65 (1972)
9. J W Bowden, M D Bolland, A M Posner J P Quirk *Nature Phys. Sci.* **245** 81 (1973)
10. M A Anderson, J F Ferguson, J Gavis *J. Colloid Interface Sci.* **54** 391 (1976)
11. D E Yates, S Levine, T W Healy *J. Chem. Soc., Faraday Trans. 1* 1807 (1974)
12. J A Davis, R O James, J O Leckie *J. Colloid Interface Sci.* **63** 480 (1978)
13. W Stumm, H Hohl, F Dalang *Croat. Chem. Acta* **48** 491 (1972)
14. R Kummert, W Stumm *J. Colloid Interface Sci.* **7** 373 (1980)
15. W Stumm, R Kummert, L Sigg *Croat. Chem. Acta* **53** 291 (1980)
16. J A Davis, J O Leckie *J. Colloid Interface Sci.* **67** 90 (1978)
17. P W Schindler, B Furst, R Dick, P Wolf *J. Colloid Interface Sci.* **55** 281 (1976)
18. P R Anderson, M M Benjamin, in *Chemical Modelling of Aqueous Systems* (Eds D C Melchior, R I Basset) (Washington, DC: American Chemical Society, 1990) p. 272
19. L Sigg, Ph.D. Thesis, Swiss National Technical University, Zürich, 1979
20. L S Balistrieri, T T Chao *Geochim. Cosmochim. Acta* **54** 739 (1990)
21. K F Hayes, A L Roe, G E Brown *Science* **23** 783 (1987)
22. D E Yates, Ph.D. Thesis, University of Melbourne, Melbourne, 1973
23. K F Hayes, J O Leckie *J. Colloid Interface Sci.* **115** 563 (1987)
24. F F Kantwell *Ion Exch. Solvent Extr.* **9** 339 (1985)
25. J Horst, Ph.D. Thesis, University and Research Centre of Karlsruhe, Karlsruhe, 1988
26. W H Höll, J Horst, M Franzreb, S H Eberle, in *Ion Exchange and Solvent Extraction, a Series of Advances* Vol. 11 (Eds J Marinsky, Y Marcus) (New York, Basel, Hong Kong: Marcel Dekker, 1993) p. 151
27. J Horst, W H Höll , S H Eberle *React. Polym.* **13** 209 (1990)
28. W H Höll, J Horst, M Wernet *React. Polym.* **14** 251 (1991)
29. W H Höll, J Horst, M Franzreb *React. Polym.* **19** 123 (1993)
30. J Horst, W H Höll *J. Colloid Interface Sci.* **195** 250 (1997)
31. W H Höll, J Horst, in *Encyclopedia of Separation Science* Vol. 2 (London: Academic Press, 2001) p. 1640
32. W H Höll *Water Sci. Technol.* **35** 287 (1997)
33. C Stöhr, Ph.D. Thesis, Karlsruhe University and Research Centre, Karlsruhe, 2001
34. W H Höll, C Stöhr *React. Funct. Polym.* **49** 117 (2001)
35. W H Höll, R Kiefer *Ind. Eng. Chem. Res.* **40** 4570 (2001)
36. W H Höll, J Horst, in *Sorbtsionnye i Khromatograficheskie Protsessy* (Sorptional and Chromatographic Processes) Vol. 1, No. 2 (Voronezh: Voronezh State University, 2001) p. 145
37. A I Kalinitchev, W H Höll, R Kifer *Zh. Fiz. Khim.* **73** 1627 (1999) [a]
38. A I Kalinitchev, W H Höll *Teor. Prak. Sorb.Prots.* (25) 44 (1999)
39. A I Kalinitchev, W H Höll *Zh. Fiz. Khim.* **74** 466 (2000) [a]
40. A I Kalinitchev, in *Problemy Khimii i Khimicheskoi Tekhnologii. Trudy VI Regional'noi Konferentsii, Voronezh 1998* (The Problems of Chemistry and Chemical Technology. Proceedings of the VIth Regional Conference, Voronezh 1998) p. T1–98
41. A I Kalinitchev, W H Höll, in *Ion Exchange at the Millennium. Proceedings of IEX 2000* (Ed. J Greig) (London: Imperial College Press, 2000) p. 201
42. A I Kalinitchev *Zh. Fiz. Khim.* **74** 1673 (2000) [a]
43. A I Kalinitchev, W H Höll, in *Trudy IX Mezhdunarodnoi Konferentsii 'Sovremennoe Sostoyanie i Perspektivy Razvitiya Teorii Adsorbtsii' (K 100-letiyu Akademika M M Dubinina)* [Proceedings of the IXth International Conference 'Modern State and Prospects for Development of Adsorption Theory (Academician M M Dubinin 100 Year Anniversary)] (Moscow: Institute of Physical Chemistry, Russian Academy of Sciences, 2001) p. 270
44. A I Kalinitchev, W H Höll, in *Sorbtsionnye i Khromatograficheskie Protsessy* (Sorptional and Chromatographic Processes) (Voronezh: Voronezh State University, 2001) Vol. 1, No. 2, p. 157
45. W H Höll, A I Kalinitchev, in *Materialy Konferentsii 'FaGran-2002' Voronezh, 2002* (Proceedings of Conference 'FaGran-2002',Voronezh, 2002) p. 26
46. A I Kalinitchev, W H Höll *Zh. Fiz. Khim.* **77** 70 (2003) [a]
47. A I Kalinitchev, W H Höll *Teor. Osnovy Khim. Tekhnol.* **37** 278 (2003)
48. A I Kalinitchev, W H Höll, in *The XYIth European Chemistry at Interfaces Conference. Book of Abstracts, Vladimir, 2003* p. 21
49. A I Kalinitchev, W H Höll, in *ICIE'03 Proceedings of International Ion Exchange Conference* (Kanazawa: Kanazawa University, 2003)
50. A I Kalinitchev, in *100 Let Khromatografii* (100 Years of Chromatography) (Ed. B A Rudenko) (Moscow: Nauka, 2003) p. 337
51. A I Kalinitchev, W H Höll *Teor. Osnovy Khim. Tekhnol.* **38** 304 (2004) [b]
52. A I Kalinitchev, W H Höll *Zh. Fiz. Khim.* **78** 1118 (2004) [a]
53. A I Kalinitchev, W H Höll, in *Ion Exchange Technology for Today and Tomorrow. Proceedings of IEX 2004* (London: Imperial College Press, 2004) p. 349
54. R M Smith, A E Martell *Critical Stability Constants* (New York: Plenum, 1976)
55. S H Eberle *Report KfK 3930UF* (Karlsruhe: Karlsruhe Nuclear Research Centre, 1986)
56. W H Höll, in *Ion Exchange Developments and Applications (Proceedings of IEX 96)* (Ed. J Greig) (Cambridge: Royal Society of Chemistry, 1996) p. 404
57. J A Marinsky *J. Chem. Phys.* **86** 3318 (1982)
58. G Klein, F Helfferich *Multicomponent Chromatography. Theory of Interference* (New York: Marcel Dekker, 1970)
59. G Klein, D Tondeur, T Vermeulen *Ind. Eng. Chem. Fund.* **6** 339 (1967)
60. A E Rodrigues, D Tondeur (Eds) *Percolation Process: Theory and Applications* (The Hague, Sijthoff and Noordhoff, 1981)
61. D M Ruthven *Principles of Adsorptions and Adsorption Processes* (New York: Wiley, 1984)
62. H Sontheimer, J C Crittenden, R S Summers *Activated Carbon for Water Treatment* (Karlsruhe: Druckerei G Braun, 1988)
63. A Kalinitchev *Ind. Eng. Chem. Res.* **34** 2625 (1995)
64. D Tondeur *Ind. Eng. Chem. Res.* **34** 2782 (1995)
65. A I Kalinitchev *Usp. Khim.* **65** 103 (1996) [*Russ. Chem. Rev.* **65** 95 (1996)
66. C Tien *Adsorption Calculations and Modelling* (Boston, London, Oxford, Singapore, Sydney, Toronto, Wellington: Butterworth-Heineman, 1998)
67. I Langmiur *J. Am. Chem. Soc.* **40** 1361 (1918)
68. M M Dubinin *Fiziko-Khimicheskie Osnovy Sorbtsionnoi Tekhniki* (Physicochemical Foundations of Sorption Equipment) (Moscow: ONTI, 1935)
69. A I Kalinitchev *Zh. Fiz. Khim.* **59** 2000 (1985) [a]
70. A I Kalinitchev *Teor. Osnovy Khim. Tekhnol.* **20** 532 (1986) [b]
71. A I Kalinitchev *Zh. Fiz. Khim.* **68** 1658 (1994) [a]
72. V G Babskii, M Yu Zhukov, V I Yudovich *Matematicheskaya Teoriya Elektroforeza* (Mathematical Theory of Electrophoresis) (Kiev: Naukova Dumka, 1983)
73. F G Helfferich, in *Migration and Fate of Pollutants in Soils and Subsoils* (Eds D Petruzzelli, F G Helfferich) (Berlin, Heidelberg: Springer, 1993)
74. F Helfferich *New Directions in Sorption Technology* (Eds G Keller, R Yang) (Boston: Butterworth, 1989)

75. F G Helfferich *AIChE Symp. Ser.* **80** 1 (1984)
76. F G Helfferich *Chem. Eng. Commun.* **44** 275 (1986)
77. V V Rachinskii *Vvedenie v Obshchuyu Teoriyu Dinamiki Sorbtsii i Khromatografii* (Introduction to General Theory of Dynamics of Sorption and Chromatography) (Moscow: Nauka, 1964)
78. E Glueckauf, in *Ion Exchange and its Application* (London: Society of Chemical Industry, 1954) p. 34
79. E Glueckauf, J I Coates *J. Chem. Soc.* **149** 1315 (1947)
80. E Glueckauf *Trans. Faraday Soc.* **51** 1540 (1955)
81. T Vermeulen, G Klein, N K Hiester, in *Perry's Chemical Engineering Handbook* (Eds R H Perry, C H Chilton) (New York: McGraw-Hill, 1973) p. 11
82. F G Helfferich *Ion Exchange* (New York: McGraw-Hill, 1962)
83. R Kiefer, Ph.D. Thesis, University and Research Centre of Karlsruhe, Karlsruhe, 1999
84. A A Samarskii, A V Gulin *Chislennye Metody* (Numerical Methods) (Moscow: Nauka, 1989)
85. M Franzreb, W H Höll, H Sontheimer *React. Polym.* **21** 117 (1993)
86. M Franzreb, W H Höll, S H Eberle *Ind. Eng. Chem. Res.* **34** 2670 (1995)
87. V Chowdiah, G Foutch, in *Ion Exchange Developments and Applications (Proceedings IEX 96)* (Ed. J Greig) (Cambridge: Royal Society of Chemistry, 1996) p. 10
88. W H Höll, J Horst, M Franzreb, in *New Developments in Ion Exchange. Proceedings of the International Conference on Ion Exchange ICIE 91* (Eds M Abe, T Kataoka, T Suzuki) (Tokyo: Kodansha, 1991) p. 279

[a] — *Russ. J. Phys. Chem. (Engl. Transl.)*
[b] — *Theor. Found. Chem. Eng. (Engl. Transl.)*